Kinetics, Spectroscopy, and Computational Chemistry of Arylnitrenes

ARTICLE *in* CHEMICAL REVIEWS · OCTOBER 2006

Impact Factor: 46.57 · DOI: 10.1021/cr040055+ · Source: PubMed

2 AUTHORS:

Nina Gritsan
Russian Academy of Sciences
166 PUBLICATIONS **2,044** CITATIONS
SEE PROFILE

Matthew S Platz
The Ohio State University
327 PUBLICATIONS **7,070** CITATIONS
SEE PROFILE

Kinetics, Spectroscopy, and Computational Chemistry of Arylnitrenes

N. P. Gritsan*,† and M. S. Platz*,‡

Institute of Chemical Kinetics and Combustion and Novosibirsk State University, 630090 Novosibirsk, Russian Federation, and Department of Chemistry, The Ohio State University, Columbus, Ohio 43210

Received October 7, 2005

Contents

Nina P. Gritsan received her Diploma in Physics from Novosibirsk State University and her Ph.D. in Chemical Physics in 1979 from the Institute of Chemical Kinetics and Combustion (Novosibirsk) of the Siberian Branch of the Russian Academy of Sciences (RAS). She was awarded the degree of Doctor of Chemistry (similar to the habilitation in Europe) at the Institute of Chemical Physics of RAS (Moscow) in 1993. Currently, she is Professor of Chemical Physics at Novosibirsk State University and head of the Laboratory of Reaction Mechanisms at the Institute of Chemical Kinetics and Combustion. Her research interests include experimental study of photochemical and photophysical processes using time-resolved and low-temperature spectroscopic techniques and the application of quantum chemistry for understanding reaction mechanisms.

Matthew S. Platz earned B.Sc. degrees in chemistry and mathematics from the State University of New York at Albany in 1973 and a Ph.D. in chemistry from Yale University in 1977 with Professor Jerome Berson. Following 18 months as a postdoctoral fellow in the laboratory of Professor Gerhard Closs at the University of Chicago, Platz joined the faculty of The Ohio State Uinversity in 1978. He was promoted to Associate Professor on 1984 and to Professor five years later. Platz served as Chair of the Chemistry Department from 1994 to 1999 and is currently Distinguished University Professor of Chemistry.

1. Introduction

Arylnitrenes are very reactive and short-lived intermediates commonly generated by decomposition of aryl azides. Although other arylnitrene precursors are known[1] and their study has led to many important mechanistic ideas, this review will be limited to studies involving only azide precursors. Aryl azides have important applications as photoresists in lithography,[2] in the formation of electrically conducting polymers,[3] in organic synthesis,[4] in photoaffinity labeling,[5] and in the covalent modification of polymer surfaces.[6] Physical organic chemists seek to understand the role of arylnitrenes in these reactions and how the structures of nitrenes control their reactivity. Spectroscopic studies of

* To whom correspondence should be addressed. (N.G.) Tel.: 7(383)333-3053. Fax: 7(383)330-7350. E-mail: gritsan@kinetics.nsc.ru. (M.S.P.) Tel.: (614) 292-0401. Fax: (614) 292−5151. E-mail: platz.1@osu.edu.
† Institute of Chemical Kinetics and Combustion and Novosibirsk State University.
‡ The Ohio State University.

10.1021/cr040055+ CCC: $59.00
Published on Web 08/23/2006

arylnitrenes have been performed in the gas phase, in low-temperature glasses and inert gas matrices, and in solution, using time-resolved methodologies. The traditional organic chemistry of aryl azides and the intermediates derived from their decomposition has been reviewed many times[4,7−13] and so will receive only limited attention in this essay.

There has been recent dramatic progress in our experimental and theoretical understanding of the arylnitrenes, primarily as a result of the application of two tools, laser flash photolysis (LFP) and high-level ab initio molecular orbital (MO) calculations.[14−17] The synergism between theory and experiment in the study of the chemistry and spectroscopy of phenylnitrene and its simple derivatives was illustrated recently.[14,17] The kinetics and spectroscopy of some substituted phenylnitrenes were considered in detail in our previous review.[16]

Interesting new results shedding light on the influence of ortho substituents on the chemistry of phenylnitrene[18−22] and on the kinetics and spectroscopy of polycylic arylnitrenes[23−25] were reported in the past few years. Moreover, the formation of vibrationally hot singlet *para*- and *ortho*-biphenylnitrenes was detected very recently[20,26] on a femtosecond time scale. The present review will attempt to highlight developments in the understanding of the spectroscopy and kinetics of arylnitrenes. This review mainly covers the experimental and theoretical discoveries of the last nine years (1997−2005). However, the most important spectroscopic and computational results, which created the basis for the interpretation of the more recent studies, will be thoroughly considered.

2. Photochemistry of Phenyl Azide and Kinetics and Spectroscopy of Phenylnitrene

Before discussing recent experimental and theoretical studies on the kinetics and spectroscopy of substituted phenylnitrenes and polycyclic arylnitrenes, we will briefly consider the photochemistry of the parent aryl azide, phenyl azide. Our purpose here is to give a brief overview to provide a context for discussion of the influence of the substituents.

2.1. Early Experimental Studies

Unfortunately, the major product obtained upon decomposition of phenyl azide (and many of its derivatives) in solution is polymeric tar.[3] A fortunate exception is the formation of azepines in the presence of primary and secondary amines. The Huisgen group[27] was the first to observe that thermolysis of **1** in the presence of aniline leads to extrusion of molecular nitrogen and formation of azepine **2a**. It was postulated that thermolysis of **1** leads to extrusion

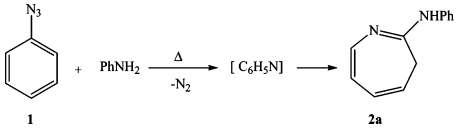

1 2a

of nitrogen and the formation of a reactive intermediate C_6H_5N. Huisgen and co-workers proposed that the trappable intermediate was either a benzazirine **4** or 1,2-didehydroazepine **5** (produced by a rearrangement of singlet phenylnitrene **3**).[27]

Later,[28] Doering and Odum demonstrated that photolysis of phenyl azide (**1**) leads to the evolution of molecular nitrogen and once again to the formation of a diethylamine-trappable intermediate (C_6H_5N) and ultimately azepine **2b**.

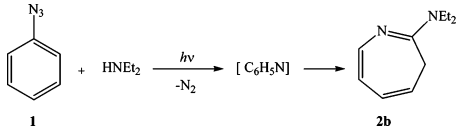

1 2b

In 1974, Wentrup[29] suggested again that the trappable intermediate might be **4** or **5**. For a long time, the nature of

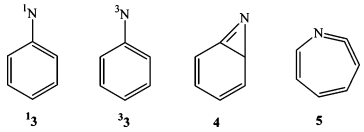

^{1}**3** ^{3}**3** **4** **5**

the intermediate(s) involved in this reaction was unclear. Candidate structures for "C_6H_5N" have been singlet (^{1}**3**) and triplet (^{3}**3**) phenylnitrene, benzazirine (**4**), and cyclic ketenimine (**5**).

Chemical analysis of reaction mixtures has provided evidence for all of these intermediates (**3**−**5**) under different conditions. High dilution of phenyl azide suppresses polymer formation,[30] and azobenzene forms, presumably due to dimerization of triplet phenylnitrenes, or in concentrated solutions by reaction of triplet phenylnitrene with phenyl azide.

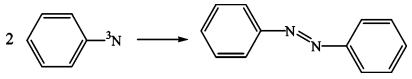

The dimerization of triplet phenylnitrene has never been directly monitored by time-resolved techniques. However, dimerization of substituted triplet phenylnitrenes (*para*-nitro[31a] and 2,4,6-tribromo[31b]), as well as polycyclic 1-naphthyl-,[32,33] 1-anthranyl-,[32] and 1-pyrenylnitrenes,[33,34] was studied by LFP techniques. The decay of triplet arylnitrenes and/or formation of corresponding azo-compounds were found to obey second-order kinetics with rate constants in the range of $(0.55-2.1) \times 10^9$ M^{-1} s^{-1} in benzene at room temperature.[31−34]

The products of nucleophilic trapping (**2**) following decomposition of **1** were initially rationalized as arising from benzazirine **4**.[27,29] This explanation was generally accepted in subsequent studies[35] and supported by calculations,[36] but in 1978, Chapman and LeRoux detected 1-aza-1,2,4,6-cycloheptatetraene (**5**) using matrix isolation IR spectroscopy.[37] The existence of the cyclic ketenimine **5** was confirmed by later spectroscopic studies in matrices[38] and in solution.[30,39,40] It was also established that ketenimine **5** is the species trapped by nucleophiles in solution to form azepines **2**.[40] Recently,[41] the low temperature ^{13}C NMR and IR spectra of **5** incorporated into a hemicarcerand were reported. The lifetime of **5** in the inner phase of a hemicarcerand was found to be 32 min at 194 K.

Experiments in matrices produced no evidence for the intermediacy of **4**.[37,38] The strongest experimental evidence to date for the intermediacy of **4** is the observation that photolysis of **1** in ethanethiol affords *o*-thioethoxyaniline (**6**) in 39% yield, presumably from the nucleophilic trapping of **4**.[42]

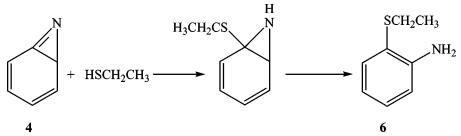

4 6

However, other interpretations of this experiment are possible. One can also propose, for example, ethanethiol trapping of 1,2-didehydroazepine **5** followed by rearrangement of the initially formed azacyclohexatriene intermediate. Thus, decisive experimental evidence in favor of **4** is not yet available.

It was found that the solution-phase photochemistry of phenyl azide (**1**) is temperature dependent.[31b] Photolysis of **1** in the presence of diethylamine at ambient temperature yields azepine **2b**. Lowering the temperature suppresses the yield of **2b** and encourages the formation of azo compound. Thus, high temperature favors reactions of singlet-state intermediates, while low temperatures favor reactions associated with triplet phenylnitrene.

The EPR spectrum of triplet phenylnitrene (^{3}**3**) was detected after photolysis of **1** in a glassy matrix, and the temperature dependence of the EPR signal demonstrated that the triplet state is the ground state of phenylnitrene.[43]

Reiser's group[44] was the first to observe the low-temperature UV−vis spectrum of triplet phenylnitrene ^{3}**3**. A later study[31b] performed in low-temperature glassy matrices revealed an additional long-wavelength band in the spectrum of ^{3}**3** (Figure 1), showing that the spectrum of ^{3}**3** reported

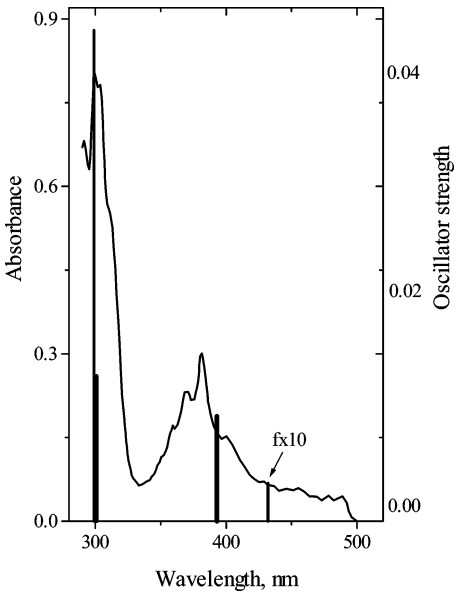

Figure 1. The absorption spectrum of triplet phenylnitrene in EPA glass at 77 K.[31b] The computed positions and oscillator strengths (*f*, right-hand axis) of the absorption bands[52] are depicted as solid vertical lines. For very small oscillator strengths, the value multiplied by 10 is presented ($f \times 10$). Reprinted with permission from ref 52. Copyright 1999 American Chemical Society.

earlier[44] was contaminated by the presence of ketenimine **5**. It was found that ^{3}**3** is extremely light sensitive, and upon photoexcitation at 77 K, ^{3}**3** rapidly isomerizes to the isomeric **5**.[31b]

Initial flash photolysis experiments involving **1** gave conflicting results with different authors favoring the presence of either triplet phenylnitrene,[45] benzazirine,[35b] or the cyclic ketenimine[30] as the carrier of the transient spectra. The currently accepted spectroscopic assignments were obtained by a combination of multiple techniques. Leyva et al.[31b] applied matrix absorption and emission spectroscopy, along with flash photolysis techniques. Chapman and LeRoux[37] obtained the matrix IR spectrum of cyclic ketenimine **5**, and Hayes and Sheridan[46] obtained the matrix IR and UV−vis spectrum of triplet phenylnitrene and cyclic ketenimine **5**. Schuster and co-workers[39,40] applied time-resolved IR and UV−vis spectroscopy to demonstrate that cyclic ketenimine **5** is formed in solution and that this species absorbs strongly at 340 nm.

In 1992, Schuster and Platz,[11] Gritsan and Pritchina,[12] and Budyka, Kantor, and Alfimov[47] wrote similar schemes, which economically explained much of the condensed-phase photochemistry of phenyl azide. UV photolysis of **1** produces singlet phenylnitrene ^{1}**3** and molecular nitrogen. In the liquid phase, ^{1}**3** isomerizes over a small barrier to form cyclic ketenimine **5**. Later computational work of Karney and Borden[48] showed this to be a two-step process involving benzazirine **4**, the species trapped by ethanethiol.

Scheme 1 represents a modern view of the mechanism of

Scheme 1

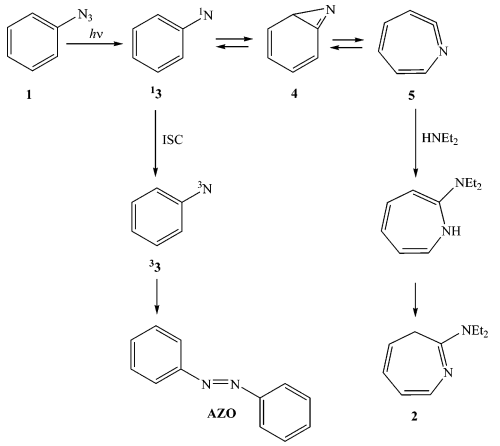

phenyl azide photochemistry. ^{1}**3** prefers rearrangement to intersystem crossing (ISC) to the lower energy triplet state at ambient temperature in the liquid phase. Below 180 K, spin relaxation (ISC) to ^{3}**3** predominates.[31b,49]

2.2. Recent Spectroscopic Observation of Singlet Phenylnitrene

The key intermediate in Scheme 1 is singlet phenylnitrene (^{1}**3**), the only intermediate that had not been detected directly or chemically intercepted prior to 1997. Gritsan, Yuzawa, and Platz[50] and the Wirz group[51] simultaneously reported that LFP of **1** or of phenyl isocyanate produces a previously undetected transient with $\lambda_{max} = 350$ nm (Figure 2) and a lifetime of ~1 ns at ambient temperature, which was assigned to ^{1}**3**.

The decay of ^{1}**3** in pentane was monitored at 350 nm over the temperature range of 150−270 K, which allowed direct measurement of the rate constant for intersystem crossing (k_{ISC}) and of accurate barriers to cyclization.[52] The formation of the products (cyclic ketenimine **5**, triplet nitrene ^{3}**3**, or both) was monitored at 380 nm.[50] The decay of ^{1}**3** and the growth of the products are first order and can be analyzed to yield an observed rate constant, k_{OBS}. An Arrhenius treatment of the k_{OBS} data (open circles) is presented in Figure 3.

The magnitude of k_{OBS} decreases with decreasing temperature until about 170 K, whereupon it reaches a limiting value of about 3.2×10^6 s^{-1}. Below this temperature, k_{OBS} remains constant.[52] The breakpoint in the Arrhenius plot is around 180−200 K and is in exactly the same temperature range where the solution-phase chemistry changes from trapping

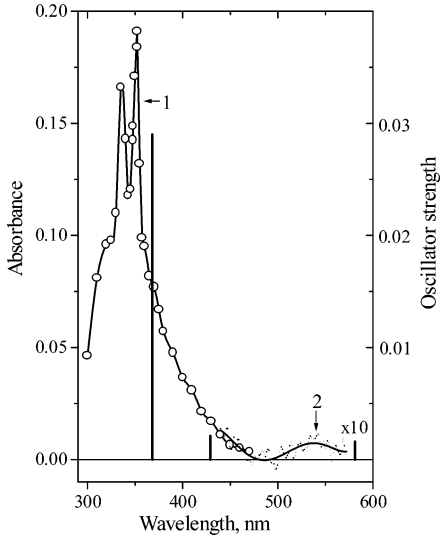

Figure 2. Transient spectrum of singlet phenylnitrene produced upon LFP of phenyl azide **1**. Spectrum 1 was recorded 2 ns after laser pulse (266 nm, 35 ps) at 233 K. The long-wavelength band (spectrum 2) was recorded with an optical multichannel analyzer at 150 K (with a 100 ns window immediately after laser pulse, 249 nm, 12 ns). The computed positions and oscillator strengths (*f*, right-hand axis) of the absorption bands are depicted as solid vertical lines.[52] For very small oscillator strengths, a value multiplied by 10 is presented ($f \times 10$).

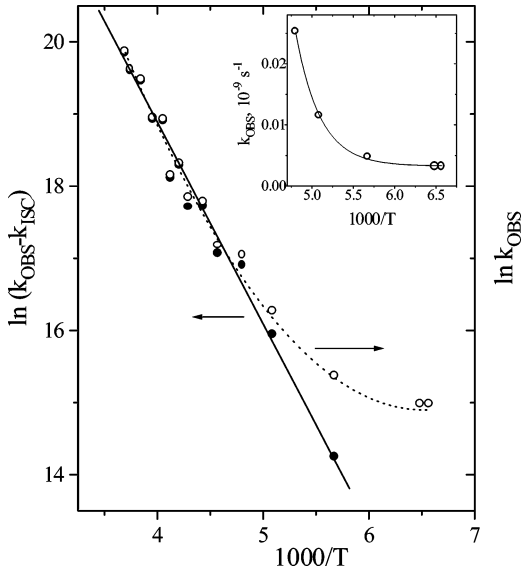

Figure 3. Arrhenius treatment of the k_{OBS} data (open circles) and k_R data (filled circles) for singlet phenylnitrene deduced upon assuming that k_{ISC} is independent of temperature.[52] Inset: temperature dependence of k_{OBS} data. Reprinted with permission from ref 14. Copyright 2000 American Chemical Society.

of ketenimine **5** with diethylamine to dimerization of ^{3}**3** to form azobenzene.[31b] Thus, the low-temperature data in Figure 3 was associated with the rate constant for ISC of ^{1}**3** to ^{3}**3** ($k_{ISC} = (3.2 \pm 0.3) \times 10^6$ s^{-1}) and the high-temperature data with k_R, the rate constant for rearrangement of ^{1}**3** (Scheme 1).

Since at any temperature $k_{OBS} = k_R + k_{ISC}$, by assuming that k_{ISC} does not change with temperature, it was possible to deduce values of k_R as a function of temperature and to obtain its Arrhenius parameters. An Arrhenius plot of $k_R = k_{OBS} - k_{ISC}$ was linear (Figure 3, solid circles), giving an activation energy for rearrangement ($E_a = 5.6 \pm 0.3$ kcal/mol) and preexponential factor ($A = 10^{13.1 \pm 0.3}$ s^{-1}).[52]

Recently,[19] the LFP of **1** was studied at 77 K where singlet nitrene ^{1}**3** cleanly relaxes to the triplet state ^{3}**3**. The spectrum of singlet phenylnitrene at 77 K was very similar to that detected in solution (Figure 2). The rate constant of ISC at 77 K was found to be $(3.8 \pm 0.3) \times 10^6$ s^{-1}.[19] Therefore, k_{ISC} for ^{1}**3** is indeed temperature independent.

2.3. Electronic Structure of Phenylnitrene

In phenylnitrene **3**, a lone pair of electrons occupies a hybrid orbital, rich in 2s character, and the two nonbonding electrons both occupy pure 2p orbitals. One of these is a p−π orbital, and the other is a p orbital on nitrogen that lies in the plane of the benzene ring. The near-degeneracy of the two 2p orbitals gives rise to four low-lying spin states—a triplet ($^3A_2$), an open-shell singlet ($^1A_2$), and two closed-shell singlets ($^1A_1$). The orbital occupancies and CASSCF-(8,8)/6-31G* geometries of three lowest spin states[48] are shown in Figure 4.

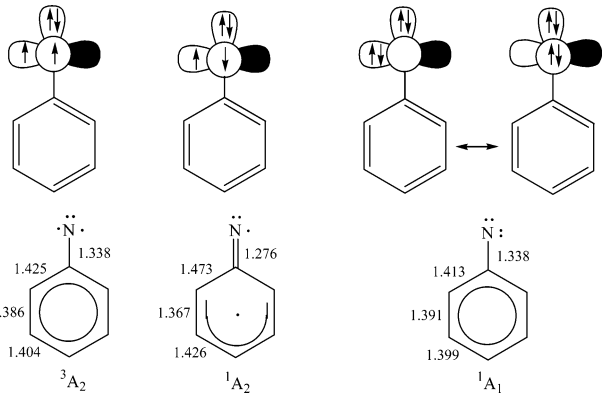

Figure 4. Orbital occupancies for nonbonding electrons and CASSCF(8,8)/6-31G* optimized geometries of the lowest triplet and singlet states of phenylnitrene.[48] Bond lengths are in angstroms. Reprinted with permission from ref 14. Copyright 2000 American Chemical Society.

In the $^3A_2$ and $^1A_2$ states, the 2p−π orbital and the in-plane 2p orbital on N are both singly occupied. The two $^1A_1$ states of **3** are a mixture of two dominant configurations—one in which the in-plane p orbital on N is doubly occupied and the 2p−π orbital is empty, which is slightly lower in energy than the configuration in which these orbital occupancies are reversed.[48,53,54] The two $^1A_1$ states differ only by a sign of this combination. In both the $^3A_2$ and $^1A_1$ states, the C−N bond is relatively long and the phenyl ring shows little bond-length alternation (Figure 4). In the $^1A_2$ state, however, strong delocalization of the electron in the nitrogen p−π orbital into the ring leads to a very short C−N bond (1.276 Å), and the bond lengths within the aromatic ring resemble those of a cyclohexadienyl radical.[48,53,54]

The $^1A_2$ state lies well below the $^1A_1$ state due to the delocalization that is present in the former state. The electron in one of the singly occupied π orbitals of the $^1A_2$ state conjugates with the π-system of the benzene ring. The second electron in a singly occupied orbital of the $^1A_2$ state remains localized in a p-orbital which lies in the plane of the aromatic ring. This confines the electron in the π-orbital and the electron of opposite-spin (resident in the in-plane 2p AO on nitrogen) to different regions of space, thus minimizing their mutual Coulombic repulsion energy.[48] Note that the open shell $^3A_2$ triplet is less sensitive to the separation of electrons than is the singlet, because of exchange stabilization.[48]

Table 1. Relative Energies (kcal/mol) of the Lowest Spin States of Phenylnitrene 3

method	electronic state $^3A_2$	$^1A_2$	$^1A_1$	ref
CISD+Q/DZ+d	0	18.3	32.4	53
σ-S,π-SDCI/6-31G*// CASSCF(8,8)/3-21G	0	18.3	38.7	54
SDCI/6-31G*/CASSCF(8,8)/3-21G	0	18.3	30.6	55
CASSCF(8,8)/6-31G*	0	17.5	42.2	48
CASPT2(8,8)/6-311G(2d,p)// CASSCF(8,8)/6-31G*	0	18.5	36.9	48
BLYP/cc-pVTZ//BLYP/cc-pVDZ	0		29.5	56
CCSD(T)/cc-pVDZ// CASSCF(8,8)/cc-pVDZ	0		35.2	56
(U)BPW91/cc-pVDZ	0	14.3		59
(U)B3LYP/6-31G*	0	14.8		60
experiment	0	18 ± 2	30 ± 5	57
	0	18.3 ± 0.7		58

The calculated[48,53−56] and experimentally determined (using gas-phase photoelectron[57] and electron detachment[58] spectroscopy) relative energies of the spin states of **3** are shown in Table 1. High levels of theory predict that the lowest singlet state ($^1A_2$) lies about 18 kcal/mol higher in energy than the triplet ground state ($^3A_2$), in excellent agreement with the experimental results.[57,58] Note that density functional theory was also applied to estimate the singlet−triplet splitting (Table 1).[59,60] The broken symmetry wave function of the $^1A_2$ state was found to have an $<S^2>$ value $\sim$ 1.0 and should be regarded as describing a 50:50 mixture of singlet and triplet states; thus, the sum method of Ziegler et al.[61] was used to estimate the energy difference between $^1A_2$ and $^3A_2$, which was found to be slightly underestimated (Table 1).

2.4. UV−Vis Spectroscopy of Singlet and Triplet Phenylnitrene

The transient spectrum of Figure 2 was assigned to singlet phenylnitrene in its lowest open shell electronic configuration ($^1A^2$ state).[50,52] This assignment was supported by the similarity of the spectrum (Figure 2) to that of the long-lived perfluorinated singlet arylnitrenes.[62] The decay of this transient absorption at ambient temperatures is accompanied by the formation of cyclic ketenimine **5**. As noted above, LFP of **1** at 77 K produces singlet nitrene ^{1}**3**, which cleanly relaxes to the triplet state ^{3}**3**. The spectrum of ^{1}**3** at 77 K is the same as that detected in solution (Figure 2).[19]

The electronic absorption spectrum of ^{1}**3** in the $^1A^2$ state calculated at the CASPT2 level is in good agreement with the transient spectrum that is observed for ^{1}**3** (Figure 2). The first two electronically excited singlet states of ^{1}**3** are both of A_1 symmetry and are predicted computationally to be at 1610 and 765 nm. Neither of these transitions has been detected because not only does excitation into both of these states have zero oscillator strength due to symmetry considerations, but these excited states are predicted to lie outside the wavelength range accessible to most spectrometers.[50,52]

The CASPT2 calculations predict a transition at 581 nm to the 1^1B_1 excited state, with a very small oscillator strength (1.6×10^{-4}), which was assigned to a very weak band with a maximum around 540 nm (Figure 2). The next excited state is the 2^1A_2 state. This transition has a small oscillator strength (2.1×10^{-3}) and an absorption maximum at 429 nm.[52]

The only intense absorption band in the absorption spectrum of ^{1}**3** is localized around 350 nm (Figure 2). The strongest absorption band in ^{1}**3**, predicted by the CASPT2 method, is the transition to the 2^1B_1 excited state, which has a 368 nm excitation energy.[52] The main configuration involved in this transition consists of an electron from the lone pair orbital on nitrogen (n_z) being promoted to the singly occupied nitrogen 2p orbital that lies in the molecular plane (p_y).

In the electronic absorption spectrum of triplet phenylnitrene ^{3}**3**, there is a strong sharp band at 308 nm, a broad structured band at 370 nm, and a broad unstructured feature, which tails out to 500 nm (Figure 1).[31b] The first calculation of this spectrum was performed by Shillady and Trindle using the INDO/S method.[36] The long wavelength maximum was calculated to be at 380 nm and was assigned to an n $\rightarrow \pi^*$ transition. The experimental long wavelength transition at about 450 nm was not reproduced by this calculation. The next transition was found to be at 330 nm and was assigned to the excitation of the nitrogen lone pair electron to the singly occupied nitrogen 2p orbital that lies in the molecular plane (p_y).

Later, Kim, Hamilton and Schaefer[53] performed configuration interaction calculations of ^{3}**3** in its ground and excited states with all single and double excitations, but they failed to reproduce the electronic absorption spectrum of triplet phenylnitrene quantitatively.

The spectrum of ^{3}**3** was very well reproduced (Figure 1) using the CASPT2 level of theory.[52] The improved correspondence is a result of the combination of an improved reference description and an adequate treatment of the dynamical electron correlation in the CASPT2 procedure.

CASPT2 calculations predict that the vertical excitation energy to the first excited state (1^3B_1) will be at 432 nm ($f = 3.4 \times 10^{-4}$). This excited state consists principally of two electronic configurations $\pi(1a_2) \rightarrow \pi(3b_1)$ and $\pi(3b_1) \rightarrow \pi_1^*(2a_2)$, where $\pi(3b_1)$ is a singly occupied π orbital. The second excited state is the 2^3A_2 state and has a vertical excitation energy of 393 nm ($f = 9.4 \times 10^{-3}$), which is associated with $\pi(2b_1) \rightarrow (3b_1)$ and $\pi(3b_1) \rightarrow \pi_2^*(4b_1)$ transitions.

The CASPT2 calculations predict that transitions to the 2^3B_1 (at 301 nm, $f = 0.013$) and 3^3B_1 (at 299 nm, $f = 0.044$) states contribute to the most intense absorption band at 308 nm. The electronic configurations for the 3^3B_1 state are the same as for the 1^3B_1 state. The main configuration involved in the $1^3A_2 \rightarrow 2^3B_1$ transition consists of excitation of an electron from the lone pair orbital (n_z) on nitrogen to the singly occupied nitrogen 2p orbital that lies in the molecular plane (p_y).

Therefore, the electronic absorption spectra of ^{1}**3** and ^{3}**3** are very similar, but all of the calculated and experimentally detected bands of ^{1}**3** (Figure 2) exhibit a red-shift compared to those of ^{3}**3** (Figure 1).[52] This is very reasonable because both of these species have very similar open-shell electronic configurations ($^3A_2$ and $^1A_2$).

2.5. Calculations on the Ring Expansion Reaction

The C_6H_5N potential energy surface originally received less attention from theoreticians than from experimentalists. Until the early 1990s, species on the reaction pathway for ring expansion of ^{1}**3** and some of its simple derivatives had been studied using only semiempirical methods.[12,36,40,63,64] MNDO calculations by the Schuster group predicted the intermediacy of azirine **4** and placed azepine **5** below **4** in energy.[40] Their calculations found barriers of 12.4 and 3.6 kcal/mol for the first and second steps of the ring expansion, respectively.[40] The much lower barrier computed for the ring

opening of **4** to **5** is consistent with the experimental finding that **5**, not **4**, is the species that is trapped in solution.[40]

Recent calculations[48] on the ring expansion of the lowest singlet state of phenylnitrene ($^1A_2$-**3**) to azacycloheptatetraene (**5**) confirm a two-step mechanism. The first step, cyclization of **^{1}3** to the azirine **4**, is predicted to be the rate-determining step. The CASPT2 energetics is depicted in Figure 5, and

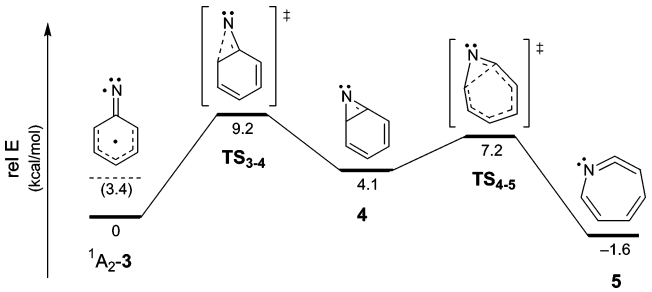

Figure 5. Energetics of the ring expansion of singlet phenylnitrene ($^1A_2$-**^{1}3**), calculated at the CASPT2(8,8)/6-311G(2d,p)//CASSCF-(8,8)/6-31G* level.[48] Correction of the energy of **^{1}3** by 3.4 kcal/mol is also displayed (see text below).

the CASSCF optimized structures of the stationary points are shown in Figure 6.

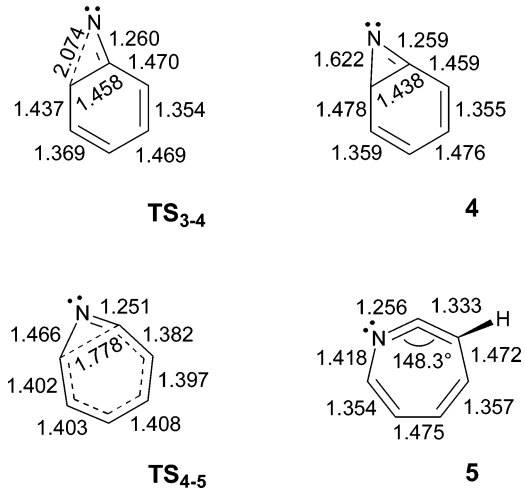

Figure 6. CASSCF(8,8)/6-31G* optimized geometries of stationary points in the ring expansion of singlet phenylnitrene ($^1A_2$-**^{1}3**).[48] Bond lengths are in angstroms, and bond angles are in degrees.

The CASPT2 calculated barrier of 9.2 kcal/mol is somewhat higher than the experimental barrier of 5.6 ± 0.3 kcal/mol.[52] The discrepancy between the calculated and experimental barrier heights is due to the general tendency of the CASPT2 method to overstabilize open-shell species (in this case, $^1A_2$-**3**) relative to closed-shell species (in this case, all the other stationary points on the reaction path).[65]

This is confirmed by comparing the CASPT2 and multireference configuration interaction (MR−CISD+Q) energy differences between open-shell singlet ($^1A''$) vinylnitrene and 2*H*-azirine.[48,66] The nitrene and azirine serve as models for $^1A_2$-**3** and **4**, respectively. This comparison with MR−CISD+Q shows that CASPT2 underestimates the energy of the open-shell nitrene reactant relative to the closed-shell 2*H*-azirine product by 3.4 kcal/mol.[48] If the relative energy of $^1A_2$-**3** is also too low by a comparable amount, then a better computational estimate of the barrier for the first step in the ring expansion of **^{1}3** would be ca. 5.8 kcal/mol, in excellent agreement with experiment.[52]

The CASPT2/6-311G(2d,p) barrier for the process **4** → **5** is only ca. 3 kcal/mol, and this reaction is calculated to be exothermic by about 5 kcal/mol (Figure 5). These computational results are consistent with the failure of Schuster's time-resolved IR experiments to detect **4**.[39,40] A 3 kcal/mol barrier implies rapid conversion of **4** to **5** at room temperature, and a 5 kcal/mol difference in energy between **4** and **5** means that at 25 °C the equilibrium would overwhelmingly favor **5**. Nevertheless, although **4** has not been observed spectroscopically, it can be intercepted by ethanethiol to form an ortho-substituted aniline.[42]

According to a recent kinetic study[41] of the decay of azepine **5** in the inner phase of a hemicarcerand, the enthalpy difference between the transition state for **^{1}3** cyclization (TS_{3-4}) and **5** was found to be 12.3 ± 0.6 kcal/mol. This estimation is in good agreement with the value 10.8 kcal/mol (Figure 5) calculated by Karney and Borden.[48]

3. Kinetics and Spectroscopy of Substituted Phenylnitrenes

After the spectrum and dynamics of parent singlet phenylnitrene **^{1}3** were measured,[50,52] our group began a comprehensive study of the substituent effect on the spectroscopy and dynamics of simple substituted phenylnitrenes. In subsequent papers,[18−20,67−71] the transient absorption spectra of a series of substituted phenylnitrenes were recorded. They are characterized by an intense absorption band in the near-UV or visible region with maxima at 340−440 nm.

Values of k_{OBS} in substituted singlet phenylnitrenes were measured by the decay of their absorption at the maxima of their spectra as a function of temperature.[18−20,67−71] As in the case of **^{1}3** (Figure 3), the magnitude of k_{OBS} decreases as the temperature decreases, until a limiting value is reached (Figure 7, 8). The temperature-independent rate constant,

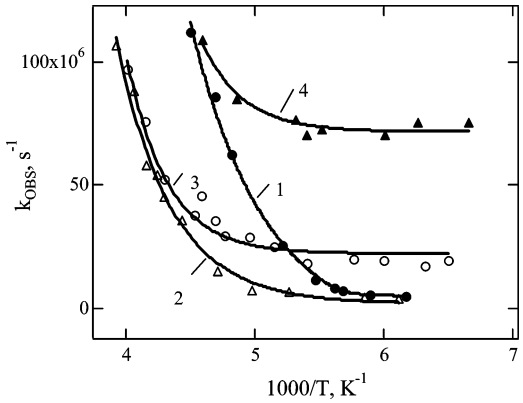

Figure 7. Temperature dependence of k_{OBS} values of *para*-fluoro (curve 1), *para*-chloro (curve 2), *para*-bromo (curve 3), and *para*-iodo (curve 4) singlet phenylnitrene in pentane. Reprinted with permission from ref 67. Copyright 1999 American Chemical Society.

observed at low temperature was associated with k_{ISC}. It is seen that in the case of *para*-bromo-, *para*-iodophenylnitrene (Figure 7), and *ortho,ortho*-dimethylphenylnitrene (Figure 8) the value of k_{OBS} is independent of temperature over a very large temperature range (∼120−200 K).

It is well-known[11−14,16,17,31b,49] that the rearrangement of singlet arylnitrenes is suppressed at 77 K and ISC becomes the only reaction at this temperature. Intersystem crossing rate constants of **^{1}3** and a series of its *ortho*-dialkyl derivatives,[19] as well as *para*- and *ortho*-biphenylnitrenes[18,20] were measured recently in glassy 3-methylpentane matrices

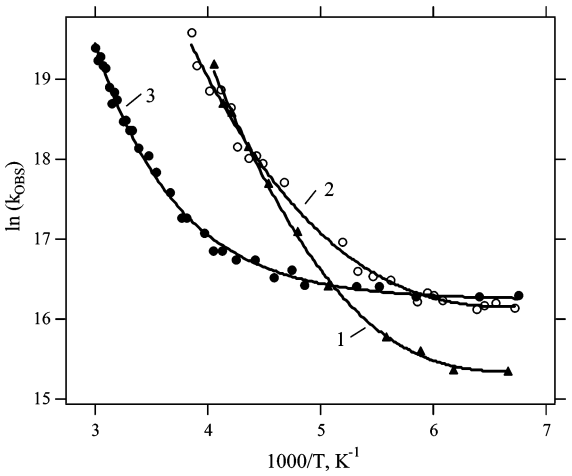

Figure 8. Arrhenius treatment of k_{OBS} values of singlet *para*-methyl (curve 1), *ortho*-methyl (curve 2) phenyl nitrene in pentane, and singlet *ortho,ortho*-dimethylphenylnitrene (curve 3) in hexane. Reprinted with permission from ref 68. Copyright 1999 American Chemical Society.

Table 2. Kinetic Parameters of Para-Substituted Singlet Aryl Nitrenes (X−C_6H_4−N) in Pentane

para-X	τ_{295K}, ns	k_{ISC} ($\times 10^6\ s^{-1}$)	E_a (kcal/mol)	log A (s^{-1})	ref
H	∼1	3.2 ± 0.3	5.6 ± 0.3	13.1 ± 0.3	52
		∼3.8[a]			19
CH_3	∼1	5.0 ± 0.4	5.8 ± 0.4	13.5 ± 0.2	67
CF_3	1.5	4.6 ± 0.8	5.6 ± 0.5	12.9 ± 0.5	67
$C(O)CH_3$	5.0	8 ± 3	5.3 ± 0.3	12.5 ± 0.3	67
F	∼0.3	3.5 ± 1.4	5.3 ± 0.3	13.2 ± 0.3	67
Cl	∼1	3.9 ± 1.5	6.1 ± 0.3	13.3 ± 0.3	67
Br	∼3	17 ± 4	4.0 ± 0.2	11.4 ± 0.2	67
I	*b*	72 ± 10	*b*	*b*	67
OCH_3	<1	>500	*b*	*b*	67
CN	8 ± 4	6 ± 2	7.2 ± 0.8	13.5 ± 0.6	70
Ph	15 ± 2	12 ± 1	6.8 ± 0.3	12.7 ± 0.3	18
		9.3 ± 0.4[a]			18
$N(CH_3)_2$[c]	0.12	8300 ± 200	*b*	*b*	72
NO_2[d]	<20	>50	*b*	*b*	73

[a] Measured at 77 K in 3-methylpentane glassy matrix. [b] Not measured. [c] In toluene. [d] In benzene.

at 77 K. Table 2 demonstrates that for ^{1}**3** and its *para*-phenyl substituted analogue values of k_{ISC} measured at 77 K and estimated from liquid-phase measurement are in very good agreement. This proves that the rate constant of intersystem crossing k_{ISC} is indeed temperature independent, as was assumed previously.[16,17,52,67−71]

3.1. Substituent Effects on Intersystem Crossing

Values of k_{ISC} for singlet para-substituted phenylnitrenes are given in Table 2. The rate constant of ISC for *para*-bromo singlet phenylnitrene is about 7 times larger than that of parent ^{1}**3** and the *para*-fluoro and *para*-chloro analogues. This is easily attributable to a small heavy atom effect. The heavy atom effect of iodine is larger than that of bromine, as expected, and increases the rate of ISC by more than a factor of 20, relative to parent ^{1}**3**.

The CH_3, CF_3, acetyl, fluoro, and chloro substituents are not sufficiently strong π donors or acceptors to significantly influence the size of k_{ISC} (Table 2). The strong π donating *para*-methoxy and *para*-dimethylamino groups have a huge influence on k_{ISC}, however. This is consistent with the solution phase photochemistry of *para*-methoxy and *para*-dimethylaminophenyl azides, which largely yield azobenzenes on photolysis.[40]

Table 3. Intersystem Crossing Rate Constants of Ortho- and Meta-Substituted Phenylnitrenes

substituent	solvent	k_{ISC} ($\times 10^6\ s^{-1}$)	ref
2-methyl	pentane	10 ± 1	68
2,6-dimethyl	pentane	15 ± 3	68
	$CF_2ClCFCl_2$	30 ± 8	68
2,6-diethyl	3-methylpentane	10 ± 2[a]	19
2,4,6-trimethyl	pentane	29 ± 3	68
	$CF_2ClCFCl_2$	20 ± 1	68
2,4,6-tri-*tert*-Bu	3-methylpentane	6.8	19
2-fluoro	pentane	3.3 ± 0.5	71
3,5-difluoro	pentane	3.1 ± 1.5	71
2,6-difluoro	hexane	2.4 ± 0.3	71
-	CCl_4	2.7 ± 0.3	71
2,3,4,5,6,-pentafluoro	pentane	3.3 ± 1.5	71
	CH_2Cl_2	10.5 ± 0.5	62
2-cyano	pentane	2.8 ± 0.3	70
2,6-dicyano	CH_2Cl_2	4.5 ± 0.5	70
	pentane	6.2 ± 0.8	70
	THF	5.9 ± 1.5	70
2-pyrimidyl	CH_2Cl_2	800 ± 200	69
2-phenyl	pentane	17 ± 1[a]	18
2-phenyl-4,6-dichloro	pentane	14 ± 1[a]	20

[a] Measured at 77 K in 3-methylpentane glassy matrix.

Table 4. Spin-Orbit Coupling Constants for the First Three Singlet States of Four Para-Substituted Phenylnitrenes (in cm^{-1})[59]

state	R = NO_2	R = F	R = H	R = NHMe
S_1	0.0	0.0	0.0	0.0
S_2	11.9	16.6	15.5	18.8
S_3	44.3	43.5	43.5	41.8

The electron withdrawing substituents (CF_3, $COCH_3$, CN, and NO_2) have a smaller but measurable influence on k_{ISC}. It is interesting to note that both electron-donating and -withdrawing substituents accelerate the ISC.

Intersystem crossing rate constants of ortho- and meta-substituted singlet phenylnitrenes are presented in Table 3. It is seen from Table 3 that mono and di-*ortho*-fluorine substituents have no influence on ISC rate constants. An *ortho*-cyano group has little influence on k_{ISC}, but two *ortho*-cyano groups slightly accelerate ISC. An *ortho*-methyl group accelerates ISC by about a factor of 3. Two *ortho*-methyl groups are more effective than one at accelerating ISC. The effect of two *ortho*-ethyl or iso-propyl groups is similar to that of methyl substituents and is about twice as large as that of two *tert*-butyl groups.[19]

Recently, Cramer and co-workers[59] calculated the electronic structures and energies of the triplet and three singlet states of **3** and of a series of its singly substituted derivatives. The spin−orbit coupling constants were calculated using the Pauli-Breit Hamiltonian to better understand the factors affecting the rates of ISC (Table 4).

For biradicals where two electrons are spatially proximate, as in nitrenes, SOC is the primary mechanism for ISC. For small amounts of SOC, the relative rate constants k_{ISC} between two systems can be estimated from the Landau−Zener model[74] as

$$\frac{k'_{ISC}}{k_{ISC}} = \left(\frac{\langle S_1|H_{SO}|T_0\rangle'}{\langle S_1|H_{SO}|T_0\rangle}\right)^2\left(\frac{\Delta E}{\Delta E'}\right)^2 \quad (1)$$

where H_{SO} is the spin−orbit coupling Hamiltonian, and ΔE is the energy difference between T_0 and S.

It was shown[59] that for all substituents except those having a σ value more negative than -0.14, a near constant T_0-S_1 energy separation (ΔE_{ST}) is predicted. Even in the case of substituents having the most negative σ values, the decrease of the energy separation does not exceed 2−3 kcal/mol.[59]

Similarly, for a series of *ortho,ortho*-dialkyl substituted phenylnitrenes, CASSCF, CASPT2, and DFT methods predict that the presence of these substituents will lower the ΔE_{ST} by only 1.5−2.5 kcal/mol.[19] Moreover, in phenylnitrenes, the SOC matrix elements between T_0 and S_1 states are required by symmetry to be zero and SOC can only be accomplished dynamically, whereby S_2 and/or S_3 character is mixed into S_1 by geometric distortion. It was concluded that the vibrationally averaged SOC matrix elements are required for a more quantitative description of the ISC in arylnitrenes.[59]

These results suggest that *ortho*-alkyl groups (Table 3) may accelerate ISC through a steric effect that forces the nitrogen atom out of the plane of the aromatic ring, thus, facilitating vibronic mixing of the low-lying singlet excited states into the lowest singlet state.

Unfortunately, there is no quantitative explanation of the pronounced effect (up to $\sim 10^3$) on the ISC rate of the strong donor substituents. According to the calculations,[59] the second term of eq 1 cannot account for a change of ISC of more than about 1.4. Cramer et al.[59] analyzed the influence of substituents on the SOC in phenylnitrene using the simplified two-electron in two-orbital configuration interaction model of Michl.[75] The strong donor substituents lead to the increase of the energy separation between two NBMO, and this in turn produce a greater mixing of S1 and upper singlet states (S2 and S3) if bonding between two NBMO appears.[59] The distortion of singlet nitrene (e.g., along the reaction coordinate for azirine formation) allows such bonding.

3.2. Substituent Effects on the Rate Constants of the Ring Expansion of Phenylnitrene

Cyclic ketenimine **5** is the major, trappable, reactive intermediate in solution when phenyl azide (at moderate concentrations) is decomposed photolytically at 298 K. The rate of decay of singlet phenylnitrene is equal to the rate of formation of the cyclic ketenimine.[50] Nevertheless the calculations of Karney and Borden[48] reveal that this is a two-step process (Scheme 1). The first step, cyclization to benzazirine **4**, is rate determining, followed by fast electrocyclic ring opening to cyclic ketenimine **5**. The predicted potential energy surface is shown in Figure 5.

In the absence of nucleophiles, the cyclic ketenimine polymerizes. At high dilution, it slowly reverts to benzazirine **4** and from there to the singlet nitrene ^{1}**3**. Eventually, the singlet nitrene relaxes to the lower energy triplet nitrene, which subsequently dimerizes.[30,40]

Until recently,[18,19,71] there was rather little direct experimental evidence for the intermediacy of **4** and its derivatives. Benzazirine **4** has not been detected by matrix IR.[37,38,46] However fluorinated,[76] naphthalenic[25,77] and *para*-amino[78] derivatives of **4** have been generated as persistent species in cryogenic matrices and characterized. Note, that azirines were detected in cases in which the barriers for ring-opening to form azepines are relatively large (Sections 3.2.2 and 4.2).

It was proposed that parent benzazirine **4** has been intercepted with ethanethiol (Section 2.1).[42] The high yield (39%) of *o*-thioethoxyaniline (**6**) upon photolysis of **1** in a net ethanethiol[42] is not in conflict with the very short lifetime of **4** in solution ($\ll$1 ns), if the rate constant of its reaction with ethanethiol is close to the diffusion limit ($\geq 10^9$ M^{-1} s^{-1}). Benzannellated derivatives of **4** have been trapped by ethanethiol[42] as well as by amines;[79,80] these results will be discussed in Section 4.1.1.

Azirine-derived products were isolated upon photolysis of a few 3,4-disubstituted phenyl azides in methanol[81] or in the presence of diethylamine.[81,82] For instance, Younger and Bell[82] isolated azirine-derived diamine (**8**) along with two azepines (**9** and **10**) upon photolysis of 3,4-diamidophenyl azide (**7**) in tetrahydrofuran (THF) in the presence of DEA.

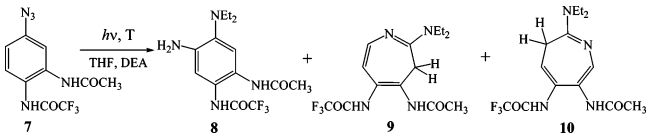

Only one azirine-derived product **8** was formed at low temperature (−70 °C), at both low (2×10^{-3} M) and high (2 M) DEA concentration. At 30 °C, only **8** was formed at high DEA concentration, but all three products (**8**−**10**) were formed at 5×10^{-3} M DEA with yields of 41, 16, and 43%, respectively. By analyzing the dependence of the product ratios, **8**/**9** and (**8**+**9**)/**10**, on the DEA concentration, Younger and Bell[82] nicely demonstrated the interconversion of a disubstituted benzazirine and singlet nitrene.

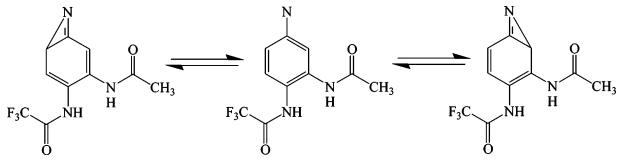

For most substituted phenyl azides of interest,[18,19,67−71] the rate constants of singlet arylnitrene decay and product formation (triplet nitrene and/or ketenimine) were found to be the same. With these arylnitrenes, cyclization to substituted benzazirines is the rate-determining step of the process of nitrene isomerization to ketenimine in a manner similar to the parent phenylnitrene (Scheme 1). A few recently discovered exceptions, *ortho*-fluorophenylnitrene,[71] *ortho*-biphenylnitrene,[18] and 2,4,6-tri-*tert*-buthylphenylnitrene,[19] will be discussed in detail in Sections 3.2.2.

The kinetics of rearrangement of substituted phenylnitrenes have been studied by LFP.[18−20,62,67−71] The temperature-independent observed rate constants are associated with k_{ISC} (Figs. 7,8). Plots of $\ln(k_{OBS}-k_{ISC})$ were linear (Figures 9−11), and these plots were used to deduce the Arrhenius parameters for cyclization of the substituted singlet arylnitrenes (Tables 2 and 5−7).

3.2.1. Influence of Para Substituents

Activation parameters of the cyclization of para-substituted singlet phenylnitrenes are presented in Table 2. It is readily seen from the table that substituents such as para CH_3, CF_3, halogen, and acetyl have little influence on k_R. This is not very surprising given that theory predicts emphatically that singlet phenylnitrene has an open-shell electronic structure.[48,53,54] Therefore, cyclization of singlet **3** requires only that the nitrogen bend out of the molecular plane, so that the singly occupied σ nonbonding molecular orbital (NBMO) can interact with the singly occupied π NBMO.[48] Azirine formation is simply the cyclization of a quinoidal 1,3-

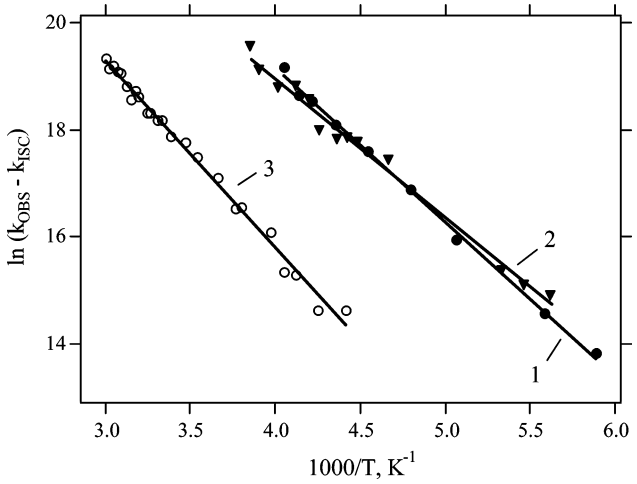

Figure 9. Arrhenius treatment of k_R (= k_{OBS} − k_{ISC}) data for singlet *para*-methyl (curve 1) and *ortho*-methyl (curve 2) phenylnitrene in pentane and for singlet *ortho,ortho*-dimethylpenylnitrene (curve 3) in hexane. Reprinted with permission from ref 68. Copyright 1999 American Chemical Society.

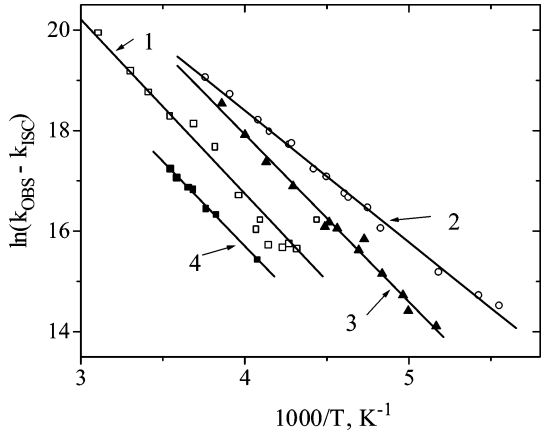

Figure 10. Arrhenius treatment of k_R (= k_{OBS} − k_{ISC}) data for singlet *para*-cyano (curve 1), *ortho*-cyano (curve 2) phenylnitrene in pentane, for singlet *ortho,ortho*-dicyanophenylnitrene in CH_2Cl_2 (curve 3)[70] and for singlet *para*-biphenylnitrene (curve 4)[18] in pentane.

biradical, which originally has two orthogonal, antiparallel spins. Thus, large substituent effects are not anticipated.

It was impossible to study the effect of strong π-donor substituents on the rate of cyclization because with *para*-methoxy and dimethylamino substituents the arylnitrene underwent ISC to the triplet nitrene faster than cyclization at all temperatures.[67]

Two para substituents, phenyl and cyano, depress k_R and retard the rate of cyclization significantly (Table 2). Phenyl and cyano are both radical stabilizing substituents. When attached to the carbon atom para to the nitrene nitrogen, these substituents concentrate spin density at this carbon and reduce the spin density at the carbons ortho to the nitrene nitrogen. The reduced spin density at carbons ortho to the nitrogen atom lowers the rate at which the 1,3-biradical cyclizes. The lifetimes of these singlet nitrenes at ambient temperature are 15 ns (phenyl) and 8 ns (cyano), and the activation barriers to cyclization are 6.8[18] and 7.2 kcal/mol,[70] respectively, compared to 5.6 kcal/mol for the unsubstituted parent **3**. The longer lifetime of singlet *para*-cyanophenylnitrene explains

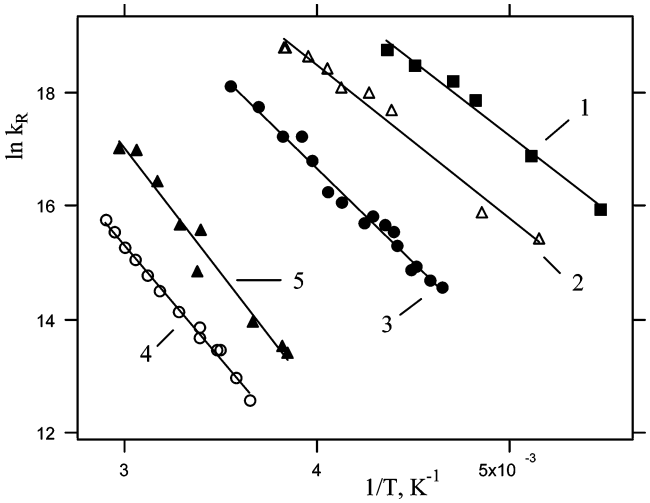

Figure 11. Arrhenius treatment of k_R (= k_{OBS} − k_{ISC}) data for singlet *para*-fluoro (curve 1), *meta,meta*-difluoro (curve 2), *ortho*-fluoromethylnitrene (curve 3) in pentane, and *ortho,ortho*-difluorophenylnitrene (curve 4) in CCl_4. Curve 5: Arrhenius treatment of the rate constant of the ring opening reaction (k_{RO}) for benzazirine **23a**. Reprinted with permission from ref 71. Copyright 2001 American Chemical Society.

Table 5. Summary of Kinetic Results for Singlet Cyano-Substituted Phenylnitrenes[70]

substituent	τ (295) (ns)	log A (s^{-1})	E_a (kcal/mol)	solvent
para-cyano, **11a**	8 ± 4	13.5 ± 0.6	7.2 ± 0.8	C_5H_{12}
ortho-cyano, **11b**	~2[a]	12.8 ± 0.3	5.5 ± 0.3	C_5H_{12}
2,6-dicyano, **11c**	~2.5[a]	13.3 ± 0.2	6.4 ± 0.3	CH_2Cl_2
	~2.3[a]	13.5 ± 0.2	6.5 ± 0.4	C_5H_{12}
	~2.3[a]	13.1 ± 1.0	6.0 ± 1.1	THF

[a] Lifetime estimated by extrapolation of the data to 295 K.

Table 6. Summary of Kinetic Results for Singlet Alkyl-Substituted Phenylnitrenes[18,68]

substituent	τ (295) (ns)	log A (s^{-1})	E_a (kcal/mol)	solvent
2-methyl, **19a**	~1[a]	12.8 ± 0.3	5.3 ± 0.4	C_5H_{12}
2,6-dimethyl, **19b**	12 ± 1	13.0 ± 0.3	7.0 ± 0.3	C_6H_{14}
	13 ± 1	12.9 ± 0.3	7.5 ± 0.5	$CF_2ClCFCl_2$
2,6-diethyl, **19c**	~9	12.1 ± 0.5	5.2 ± 0.5	C_5H_{12}
2,4,6-trimethyl, **19d**	8 ± 1	13.4 ± 0.4	7.3 ± 0.4	$CF_2ClCFCl_2$
4-methyl, **19e**	~ 1[a]	13.2 ± 0.2	5.8 ± 0.4	C_5H_{12}

[a] Lifetime estimated by extrapolation of the data to 295 K.

the high yield (>70%) of hydrazine (**14a**) observed upon photolysis of *para*-cyanophenyl azide in dimethylamine.[84]

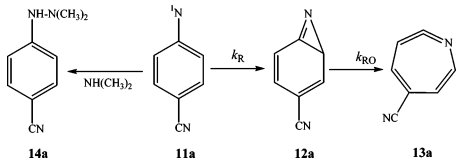

To test the validity of these qualitative expectations, CASPT2/6-31G* calculations on the ring expansion reactions of singlet *para*-cyanophenylnitrene (**7a**) were performed.[70] Table 8 shows that the barrier for cyclization of **11a** is more than 1 kcal/mol higher than that for parent phenylnitrene **3**. This is in quantitative agreement with experiment (Table 5).

Recently, Cramer and coauthors[59] performed calculations of the ring expansion reaction for three para-substituted

Table 7. Kinetic Parameters of Fluoro-Substituted Singlet Phenylnitrenes[62,71,83]

substituent	τ_{298} (ns)	log A (s^{-1})	E_a (kcal/mol)	solvent	ref
H	~1	13.1 ± 0.3	5.6 ± 0.3	C_5H_{12}	52
2-fluoro, **22a**	8 ± 1	13.0 ± 0.3	6.7 ± 0.3	C_5H_{12}	71
	10 ± 2			CH_2Cl_2	71
	10 ± 2			$CF_2ClCFCl_2$	71
4-fluoro, **22b**	~0.3	13.2 ± 0.3	5.3 ± 0.3	C_5H_{12}	71
3,5-difluoro, **22c**	~3	12.8 ± 0.3	5.5 ± 0.3	C_5H_{12}	71
2,6-difluoro, **22d**	240 ± 20	11.5 ± 0.5	7.3 ± 0.7	C_6H_{14}	71
	260 ± 20	12.0 ± 1.2	8.0 ± 1.5	CCl_4	71
2,3,4,5,6-	56 ± 4	12.8 ± 0.6	7.8 ± 0.6	C_5H_{12}	71
pentafluoro, **22e**	32 ± 3	13.8 ± 0.3	8.8 ± 0.4	CH_2Cl_2	62
perfluoro-4-	260 ± 10	13.2 ± 0.2	9.4 ± 0.4	CH_2Cl_2	62
biphenyl, **22f**	220 ± 10	12.5 ± 0.4	8.9 ± 0.3	CH_3CN	83
4-$CONHC_3H_8$-2,3,5,6-tetrafluoro, **22g**	210 ± 20	13.2 ± 0.3	7.5 ± 0.3	CH_3CN	83

Table 8. (8/8)CASSCF and CASPT2/6-31G* Energies (kcal/mol)[a] Relative to the Reactants, for the Transition Structures and Products in the Cyclization Reactions of Singlet Phenylnitrene and of the *para*-, *ortho*-, *meta*-, and 2,6-Dicyano Derivatives[70]

			CASSCF		CASPT2	
substituent	cyclization mode[b]	azirine	TS	product	TS	product
H		**4**	8.9	4.7	8.6	1.6
para-cyano, **11a**		**12a=12a′**	9.4	5.0	9.8	3.3
ortho-cyano, **11b**	away from	**128b**	8.3	4.5	8.6	2.2
	toward	**12b′**	8.4	2.6	7.5	0.3
ortho,*ortho*-dicyano, **11c**		**12c=12c′**	8.2	3.1	8.0	1.5
meta-cyano, **11d**	away from	**12d**	8.6	4.4	8.2	1.2
	toward	**12d′**	8.1	2.9	7.6	−0.7

[a] Including zero-point energy (ZPE) corrections, which range from −0.3 to 0.1 kcal/mol for transition structures and from 0.9 to 1.4 kcal/mol for products. [b] Mode of cyclization, toward or away from the substituted carbon.

Table 9. CASPT2 Enthalpies (H_{298}, kcal/mol) of Stationary Points Relative to the Singlet Arylnitrenes (15) for Different Para Substituents R[59] [a]

R	TS1	**16**	TS2	**17**
$NHCH_3$, **15a**	12.3	8.5	13.3	1.7
H, **15b=3**	8.5	2.7	5.8	−1.9
F, **15c**	8.9	3.0	7.3	−1.6
NO_2, **15d**	9.5	3.7	4.8	−0.7

[a] All structures were optimized at the CASSCF(8,8)/cc-pVDZ level.

singlet phenylnitrenes with substituents that range from highly electron-donating (**15a**, $NHCH_3$) to highly electron-withdrawing (**15d**, NO_2).

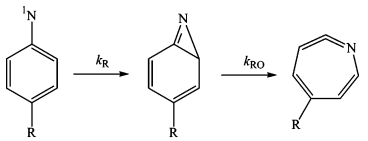

15a-d **16a-d** **17a-d**

They optimized structures for the stationary points at the BPW91, BLYP, and CASSCF levels of theory. Table 9 gives data from only the most accurate calculations, those performed at the CASPT2/CASSCF level of theory.[59]

The calculations found that in the case of F and NO_2 substituents, as in the case of the parent system, cyclization is weakly exothermic, and the formation of azirine (**16**) is the rate-determining step. In the case of the highly electron-withdrawing NO_2 substituent, the barrier for cyclization was calculated to be 1 kcal/mol higher than that for parent phenylnitrene **3**.[59]

Unfortunately, it was impossible to measure the rate constant of cyclization of **15d** due to its very fast rate of ISC.[67] No trace of the 3*H*-azepine was reported among the products of *p*-nitrophenyl azide (**18**) photolysis in neat dimethylamine[84a] or diethylamine.[40] At the same time, photolysis of **18** in diethylamine gives a hydrazine product in 9% yield.[73] The latter fact indicates that the lifetime of **15d** is not extremely short. This finding is consistent with the absence of azepine only if the cyclization reaction is suppressed (Table 9).

For the NHMe-substituted case, ring expansion was predicted to be weakly endothermic, and electrocyclic ring-opening of **16a** was predicted to be the rate-determining step.[17] The barrier to the cyclization of **15a** was found to be about 4 kcal/mol higher than that of the parent system **3**.[59] The predicted reduction of the reactivity, along with much faster ISC ($k_{ISC} = (8.3 \pm 0.2) \times 10^9$ s^{-1}) than in parent **3**, accounts for the absence of 3H-azepines as products of *para*-dimethyaminophenyl azide photolysis in the presence of nucleophiles.[73]

3.2.2. Influence of Ortho Substituents

3.2.2.1. *ortho*-Alkyl Substituents. Photolysis of several *ortho*-alkyl aryl azides (e.g., *o*-methyl, *o*-ethyl, and *o*-isopropyl) in diethylamine affords nucleophilic trapping products that are consistent with initial cyclization of singlet nitrene to the unsubstituted ortho carbon only.[85]

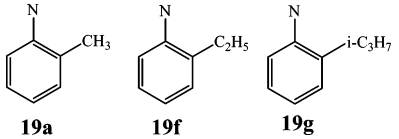

19a **19f** **19g**

Murata and Tomioka have observed the tetracyanoethylene trapping of singlet 2,4,6-tri-methylphenylnitrene (**19d**), as well as of its ring-expansion product.[86] These results[85,86] demonstrate that steric effects play a role in determining the barrier to ring expansion.

Table 10. Kinetic Parameters in Pentane for the Second Step of the Singlet Arylnitrene Isomerization, the Ring-Opening Reaction[18,19,71]

substituent	τ_{298} (ns)	log A_{RO} (s^{-1})	E_{RO} (kcal/mol)	ref
2,4,6-tri-*tert*-buthyl, **19i**	62 ± 2	12.6 ± 0.2	7.4 ± 0.2	19
2-fluoro, **22a**	100 ± 10	13.5 ± 0.4	9.0 ± 0.5	71
2-phenyl, **28a**	13 ± 1	12.1 ± 0.1	5.7 ± 0.2	18
28a-d_9	11 ± 1	12.6 ± 0.1	6.3 ± 0.1	18

Note that the related cyclization of singlet nitrene to the unsubstituted ortho carbon only was observed in the case of *o*-flurophenylnitrene.[87] The singlet *ortho*-cyano[70,88] and *ortho*-acetylphenylnitrenes[89] undergo cyclization not only away from the substituent but also toward the cyano or acetyl group. As will be discussed in Sections 3.2.2.2 and 3.2.2.3, both steric and electronic effects play important roles in these cases.

As was written in Section 3.2, for most substituted phenylnitrenes[18,19,67−71] cyclization to substituted benzazirines is the rate-determining step of the process of nitrene isomerization to ketenimine, similar to that of the parent singlet phenylnitrene ^{1}**3**.

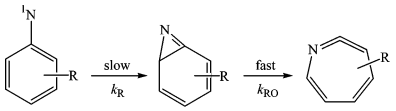

For these arylnitrenes, the Arrhenius parameters for the cyclization reaction are presented in Tables 5−7. However, for a few ortho-substituted phenylnitrenes (namely, *ortho*-fluorophenyl-, *ortho*-biphenyl-, and 2,4,6-tri-*tert*-butylphenylnitrene), the ring-opening reaction was found to be the rate-limiting step.[18,19,71] Therefore, for these nitrenes the Arrhenius parameters for the ring-opening reaction (k_{RO}, A_{RO}, E_{RO}) could be obtained (Table 10).

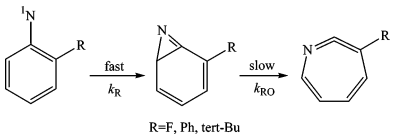

A recent kinetic study[68] demonstrated that a single ortho (**19a**) (as well as para, **19e**) methyl substituent has no influence on the rate of cyclization of the singlet tolylnitrene to the azirine (Table 6). In contrast to the case of **19a**, cyclization of di-*ortho*-methyl-substituted nitrenes **19b**,**d** necessarily proceeds toward a carbon bearing a substituent. It was found that in the case of **19b** the resulting steric effect raises the barrier to cyclization by 1.5−2.0 kcal/mol,[68] in quantitative agreement with the results of CASPT2 calculations of Karney and Borden,[90] who predicted that the barrier to rearrangement of **19a** away from the methyl group is 2 kcal/mol lower than toward the methyl group. The steric effect extends the lifetime of **19b** at ambient temperature to 12 ns in pentane.[68]

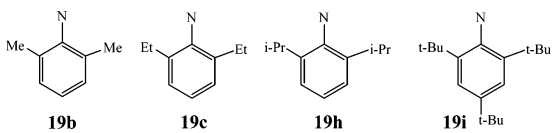

Taking into account the pure steric effect of the methyl substituent, it would be possible to expect even longer lifetimes of singlet arylnitrenes with bulky substituents in the ortho position (**19c**, **19h**, **19i**). However, the experimental results are opposite to this expectation.[19] The lifetimes of the nitrenes **19c** and **19h** were found to be shorter than that of **19b**, and singlet nitrene **19i** was not observed in liquid solution due to its very short lifetime. However, the benzazirine **20i** was detected ($\lambda_{max} = 285$ nm, Figure 12, spectrum

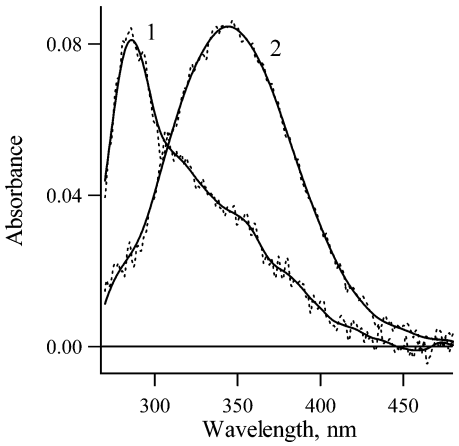

Figure 12. Transient absorption spectra produced upon LFP (266 nm) of 2,4,6-tri-*tert*-butylphenyl azide in pentane at ambient temperature over a window of 10 ns just after the laser pulse (1) and 1 μs after the laser pulse (2).

1) and proven to be a precursor of ketenimine **21i** ($\lambda_{max} =$ 350 nm, Figure 12, spectrum 2). Therefore, it was possible to measure the barrier for its ring-opening reaction (Table 10).[19]

To understand the origin of the alkyl substituent effects, the intramolecular rearrangement of phenylnitrenes with 2-methyl (**19a**), 2-isopropyl (**19g**), 2-*tert*-butyl (**19j**) substituents were investigated computationally.[19] It was found that the energy barriers to cyclization for nitrenes **19g** and **19j** away from alkyl substituents are unsurprisingly smaller than those to cyclization toward them and are diminished as the size of the alkyl group increases. The barrier for nitrene **19j** to cyclization toward the *tert*-butyl group is only 0.4 kcal/mol higher than that of phenylnitrene ^{1}**3**. In turn, the barrier to cyclization away from the *tert*-butyl group is 3.6 kcal/mol lower than that of ^{1}**3**. The origin of the dramatic drop of the barrier is the strain released between the nitrogen atom and the alkyl substituent when the nitrogen atom moves away from substituent during the cyclization (Scheme 2).[19]

Scheme 2

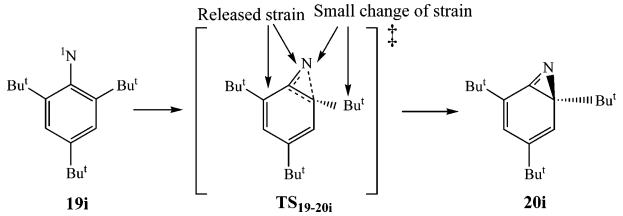

Theory predicts that the bulkiness of alkyl substituents will alter not only the energy barrier of the first cyclization step but the second ring-expansion step as well. The computational data indicate that the bulkier alkyl substituents have the higher activation energy for the second step.[19] Results of calculations evidently showed that the bulkiest *tert*-butyl substituent dramatically reduces the energy barrier of the first cyclization step and raises the barrier of the second ring-expansion step. Therefore, in this case the rate-determining step is the second ring-expansion reaction as was found

experimentally.[19] Note that the calculated barrier (6.3 kcal/mol) is very close to the experimentally determined activation energy of this reaction (E_{RO} = 7.4 ± 0.2 kcal/mol, Table 10).[19]

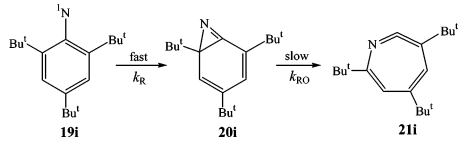

3.2.2.2. *ortho*-Cyano Substituents. A cyano group is a smaller substituent than methyl and also should localize an unpaired electron at the carbon where this substituent is attached. Thus, cyclization toward and away from the substituted ortho carbon should be more evenly balanced for a cyano than for an alkyl substituent. Consistent with this hypothesis, the Smalley group[88] found that singlet *ortho*-cyanophenylnitrene **11b** undergoes ring expansion to afford not only **13b**, the product formed by cyclization away from the cyano substituent, but also **13b′**, the product formed by cyclization toward the cyano group (Scheme 3). Similar

Scheme 3

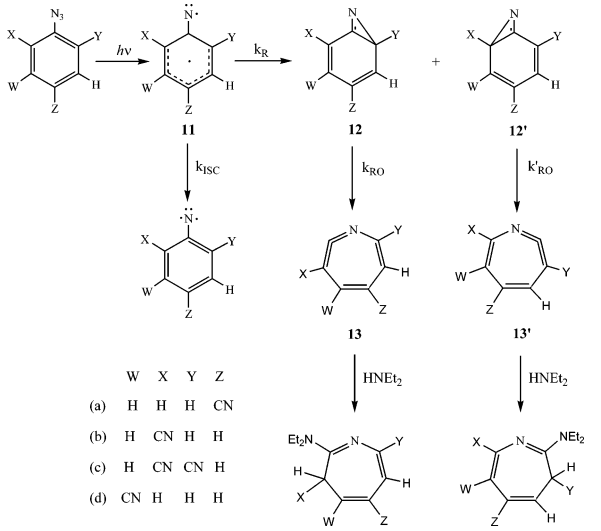

results have been found in the ring expansion of singlet *ortho*-acetylphenylnitrene.[89]

Laser flash photolysis studies were performed on *ortho*-cyano (**11b**) and *ortho,ortho*-dicyano phenylnitrene (**11c**).[70] The results are given in Table 5. In pentane the barrier to cyclization of *ortho*-cyanophenylnitrene is the same, within experimental error, to that of parent phenylnitrene. The barrier to cyclization of *ortho,ortho*-dicyanophenylnitrene (**11c**) is about 1 kcal/mol larger than that of parent phenylnitrene (**^{1}3**). Variation of solvent has only a small effect on the kinetics of this nitrene.

Product studies demonstrated that *ortho*-cyanophenylnitrene (**11b**) slightly prefers to cyclize toward the carbon bearing the cyano group (63:37) in pentane solvent.[70] Thus, the spin localization effect and the steric effect of cyano, relative to hydrogen, essentially cancel, and there is no net influence of the substitutent on the reaction barrier. The barrier to cyclization of *ortho,ortho*-dicyanophenylnitrene **11c** increases, but the increase is smaller than that found for 2,6-dimethylphenylnitrene (**19b**).

The qualitative predictions and experimental findings in the case of cyano substituents have been analyzed computationally by performing (8/8)CASSCF and CASPT2/6-31G* ab initio calculations (Table 8).[70] Table 8 summarizes the results for the cyclization reactions of *para*-, *ortho*-, and *meta*-cyanophenylnitrenes and *ortho,ortho*-dicyanophenylnitrene (**11a**−**d**). The zero-point corrected energies of the two possible products, **12** and **12′**, are given, relative to the reactants. Also shown are the relative energies of the transition structures, TS (**11** → **12**) and TS (**11** → **12′**), leading to each of the products. For comparison, the CASSCF and CASPT2 relative energies for the cyclization reactions of unsubstituted **^{1}3** are given as well.[48]

CASSCF and CASPT2 calculations both overestimate the stability of the open-shell electronic structure of singlet nitrenes **11a**−**d** by about 3 kcal/mol,[70] as in the case of parent **^{1}3**.[48] The ring opening is computed to require passage over a 2−3 kcal/mol lower energy barrier than reversion of the intermediates to the reactants. Therefore, cyclization is the rate-determining step in the ring expansion reactions of cyano-substituted phenylnitrenes **11a**−**d** to **13** and **13′** (Scheme 3).

Of particular interest in Table 8 are the results for cyclization of *ortho*-cyanophenylnitrene (**11b**). Cyclization of **11b** toward the cyano substituent was predicted to have a slightly lower barrier height than cyclization away from the cyano group, which is calculated to have the same barrier height as cyclization of **^{1}3** at the CASPT2 level of theory. These results are in accord with experimental data on the product ratio (63:37) and the experimental activation energy (Table 5).[70]

3.2.2.3. *ortho*-Fluoro Substituents. Abramovitch, Challand and Scriven[91,92] and the Banks group[93−96] discovered that unlike most arylnitrenes, polyfluorinated arylnitrenes have bountiful bimolecular chemistry. Polyfluorinated arylnitrenes are useful reagents in synthetic organic chemistry,[97] in photoaffinity labeling,[98−105] and for the covalent modification of polymer surfaces.[6] The effects of the number and positions of fluorine substituents on the ring expansion of phenylnitrene have been extensively investigated by members of the Platz group.[97,106−110] They concluded that fluorine substitution at both ortho positions is required to inhibit ring expansion effectively.

To understand the fluorine effect quantitatively, the kinetics of fluoro-substituted phenylnitrenes (Scheme 4) was studied,[71] and the data were interpreted with the aid of molecular orbital calculations.[71,90]

Scheme 4

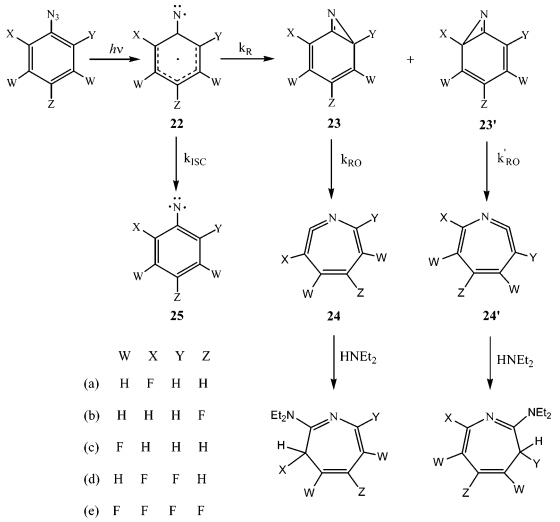

Table 11. Calculated Relative Energies (kcal/mol)[a] for Species Involved in the First Step of the Ring Expension of Fluorosubstituted Phenylnitrenes[71,90]

substituent		mode	CAS/6[b]	PT2/6[c]	PT2/cc[d]
H	**3**		0	0	0
	TS		8.9	8.6	9.3
	4		4.7	1.6	3.5
	22a		0	0	0
2-F	TS1	away	9.5	9.5	9.9
	23a		6.1	3.6	4.8
	TS2	toward	13.6	12.3	13.0
	23a′		0.7	−2.4	−0.3
	22b		0	0	0
4-F	TS		7.9	8.5	9.1
	239b		3.3	1.6	3.3
	22c		0	0	0
3,5-diF	TS		8.5	7.9	8.6
	23c		3.2	−0.7	1.1
	22d		0	0	0
2,6-diF	TS		13.9	13.0	13.4
	23d		2.1	−0.5	1.0

[a] Energies pertain to CASSCF(8,8)/6-31G* optimized geometries. [b] CASSCF(8,8)/6-31G* energy. [c] CASPT2N/6-31G* energy. [d] CASPT2N/cc-pVDZ energy.

Placement of fluorine substituents at both ortho positions (**22d**) raises the barrier to cyclization by about 3 kcal/mol, relative to the unsubstituted system (Table 7). This is consistent with the calculations of Karney and Borden,[90] who found that cyclization *away* from an *ortho*-methyl or an *ortho*-fluorine group is favored by 2−3 kcal/mol relative to cyclization *toward* the substituent.

The work of Leyva and Sagredo[87] demonstrated, in fact, that cyclization of the singlet nitrene **22a** proceeds away from the fluorine substituent. The steric argument predicts that a single *ortho*-fluorine substituent will have little influence on the rate of conversion of **22a** to **23a**, since cyclization occurs at the unsubstituted ortho carbon.

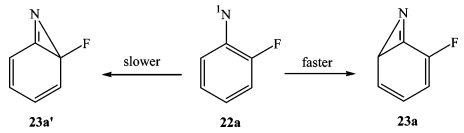

However, the barrier to this process is larger (outside of experimental error) than that of the parent system (Table 7). In fact, the lifetime of singlet 2-fluorophenylnitrene (**22a**) at 298 K is 8−10 times longer than that of the parent (**^{1}3**). Therefore, a single *ortho*-fluorine atom exerts a small but significant bystander effect on remote cyclization that is not simply steric in origin. This result is in good quantitative agreement with the computational data of Karney and Borden,[90] who predicted that the barrier to cyclization of **22a** *away* from the fluorine substituent is about 1 kcal/mol higher than that for parent system **^{1}3** (Table 11).

To understand this substituent effect, the atomic charges for the different centers were computed.[71] It was found that fluorine substitution makes the adjacent carbon very positively charged (+0.48 e). In the transformation of **22a** to TS1 (away from F) or TS2 (toward F), there is an increase in positive character at the (ipso) carbon bearing the nitrogen. The increased activation barrier to cyclization for **22a** relative to **^{1}3** is due to the build up of positive charges on the ortho and ipso carbons in TS1 for cyclization of **22a**.

For insertion toward F in TS2 there is an even greater amount of positive−positive charge repulsion between the ortho and ipso carbons than in TS1, and this effect is responsible, in part, for a higher activation barrier for insertion toward F than away from F. Therefore, the origin of the influence of *ortho*,*ortho*-difluoro substitution on prolonging the lifetime of singlet arylnitrene and increasing the activation energy for cyclization is due to a combination of the steric effect and the extraordinary electronegativity of the fluorine atom. In this case, the electronic and steric effects reinforce each other. This is the opposite of the case of *ortho*,*ortho*-dicyanophenylnitrene (**11c**), where the electronic and steric effects oppose and nearly cancel each other.

Unique kinetic results were obtained upon LFP of *ortho*-fluorophenyl azide.[71] In this case the decay of **22a** was much faster than the formation of products (ketenimine **24a** and triplet nitrene **25a**) at temperatures above 230 K (Figure 13).

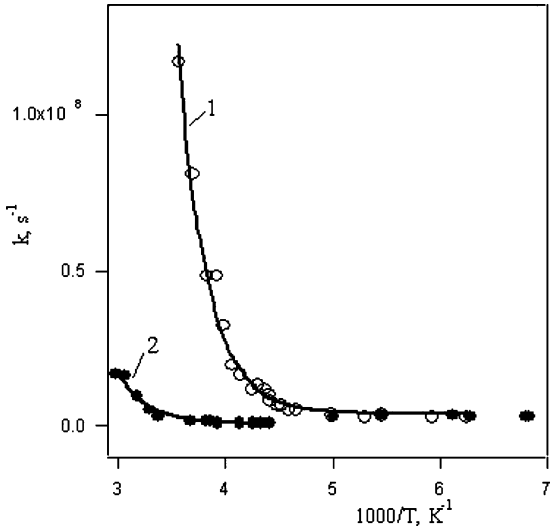

Figure 13. The temperature dependence of the rate constant of decay of singlet *ortho*-fluorophenylnitrene **22a** (curve 1) and the apparent rate constant of formation of triplet 2-fluorophenylnitrene **25a** and ketenimine **24a** (curve 2). Solid lines (1) and (2): results of nonlinear global fit of the data to analytical solution according Scheme 5. Reprinted with permission from ref 71. Copyright 2001 American Chemical Society.

Between 147 and 180 K, the rate constant for the growth of the triplet is equal to the rate constant for the disappearance of **22a**, and both rate constants are temperature-independent and close to the value of k_{ISC} for parent **^{1}3**. In this temperature range (147−180 K), singlet nitrene **22a** cleanly relaxes to the lower energy triplet nitrene **25a**.

Above 180 K, **22a** decays by both intersystem crossing (k_{ISC}) and cyclization (k_R), with the latter process gaining relative to the former as the temperature increases. The data for temperatures above 180 K were explained by positing that singlet nitrene **22a** and azirine **23a** (Scheme 5) interconvert under the experimental conditions.[71]

Kinetic data for singlet *ortho*-fluoronitrene **228a** were analyzed[71] following Scheme 5. The equilibrium constant K_R ($K_R = k_{-R}/k_R$) was estimated to be about 0.5 and ΔG to be ∼350 cal/mol. Thus, **22a** and **23a** are very close in energy. The rate constant, k_{RO}, for the ring opening reaction was measured, and the Arrhenius parameters were found to be $A_{RO} = 10^{13.5\pm0.4}$ M^{-1} s^{-1} and $E_{RO} = 9000 \pm 500$ cal/mol (Table 10).

To test, computationally, the proposed explanation of the unique kinetics observed for **22a**, a series of ab initio and density functional theory (DFT) calculations on the second step of the ring expansion were performed (Table 12).[71] The

Scheme 5

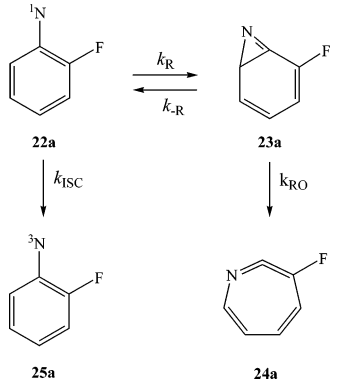

Table 12. Relative Energies (in kcal/mol)[a] and Zero-Point Vibrational Energies of Azirines 23, Ketenimines 24, and the Transition States (TS) Connecting Them[b]

	azirine		transition state		ketenimine	
method	E	ZPE	rel E	ZPE	rel E	ZPE
	4		**TS**		**5**	
CASPT2/cc-pVDZ[c]	−285.41815	60.9	2.5	59.8	−4.5	60.8
B3LYP/6-31G*[d]	−286.27659	57.7	4.7	56.7	−5.1	57.6
	23a		**TSa**		**24a**	
CASPT2/cc-pVDZ[c]	−384.47462	55.7	7.0	54.6	−1.6	55.8
B3LYP/6-31G*[d]	−385.50238	52.8	8.1	51.7	−3.0	52.8
B3LYP/6-311+G(2d,p)[d]	−385.62115		7.0		−5.5	
CCSD(T)/6-31+G*[d]	−384.48202		11.2			
	23a′		**TSa′**		**24a′**	
CASPT2/cc-pVDZ[c]	−384.48308	55.9	2.4	54.8	−6.0	55.7
B3LYP/6-31G*[d]	−385.51174	52.7	4.1	51.8	−6.8	52.8
	23b		**TSb**	**24b**		
CASPT2/cc-pVDZ[c]	−384.48077	55.6	4.5	54.5	−4.3	55.5
B3LYP/6-31G*[d]	−385.50865	52.6	5.7	51.5	−5.5	52.6
	13c		**TSc**		**24c**	
CASPT2/cc-pVDZ[c]	−483.52115	50.5	5.2	49.3	−2.7	50.3
B3LYP/6-31G*[d]	−484.74392	47.7	6.4	46.6	−3.9	47.6
	13d		**TSd**		**24d**	
CASPT2/cc-pVDZ[c]	−483.51566	50.7	5.7	49.6	−3.7	50.6
B3LYP/6-31G*[d]	−484.73747	47.8	6.8	46.8	−5.1	47.9
	13e		**TSe**		**24e**	
B3LYP/6-31G*[d]	−382.41002	32.6	8.5	31.5	−6.0	32.6

[a] Reprinted with Permission from ref 71. Copyright 2001 American Chemical Society. [b] Azirine energies are absolute energies, in hartree. Energies for transition states and ketenimines are relative energies, compared to the azirine, and are corrected for differences in zero-point vibrational energy. [c] Obtained using CASSCF(8,8)/6-31G* optimized geometry and zero-point vibrational energy. [d] Obtained using B3LYP/6-31G* optimized geometry and zero-point vibrational energy.

CASPT2 results are depicted graphically in Figure 13, in a way that permits energetic comparisons of isomeric species.

As shown in Figure 14, in all cases except the "away" ring expansion of 2-fluorophenylnitrene (**22a**), the transition state for the second step of the ring expansion (**23** → **24**) is computed to be lower in energy than that for the first step (**22** → **23**) at the CASPT2 level of theory. This is consistent with the experimental finding that, for all other fluorinated phenylnitrenes, the nitrene decays at the same rate at which the corresponding ketenimine is formed, whereas for nitrene **22a**, nitrene decay is faster than ketenimine growth.

Curiously, the addition of a second *ortho*-fluorine substituent (i.e., in benzazirine **23d**) raises the barrier to reversion to singlet nitrene **22d**, relative to the mono *ortho*-fluoro system (Figure 14). This is partly due to steric hindrance by fluorine in the transition state for cyclization but is also due to the stabilization of **23d** by the fluorine attached directly to the azirine ring (vide supra).[71] The addition of the second

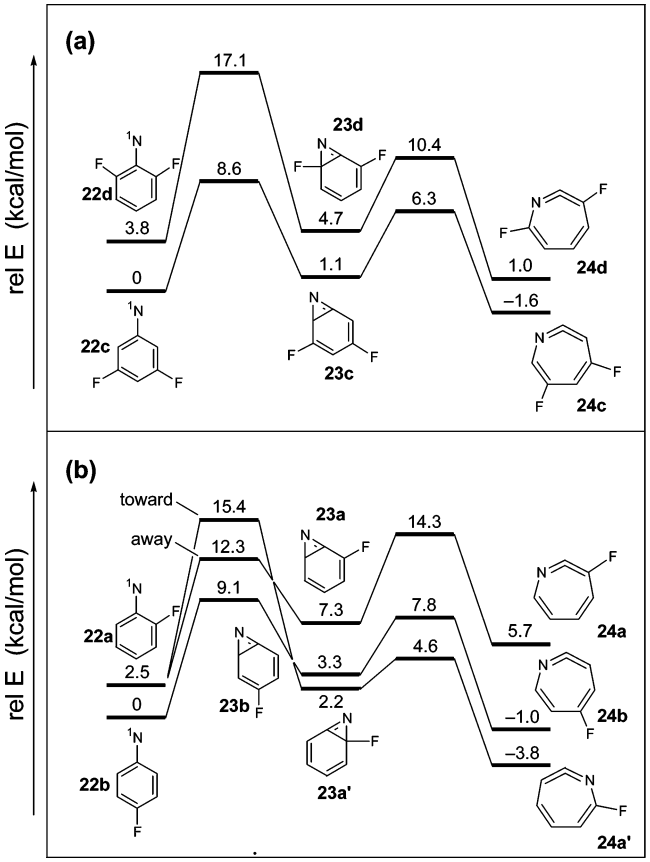

Figure 14. Relative energies (in kcal/mol)[71,90] of species involved in the ring expansions of singlet fluoro-substituted phenylnitrenes calculated at the CASPT2/cc-pVDZ//CASSCF(8,8)/6-31G* level. (a) Difluorinated phenylnitrenes. (b) Monofluorinated phenylnitrenes. Reprinted with permission from ref 71. Copyright 2001 American Chemical Society.

fluorine substituent (benzazirine **23d**) decreases the barrier to conversion of azirine **23d** to ketenimine **24d** slightly (Figure 14). This is related to the more favorable thermodynamics of conversion in the case of **23d** compared with **23a**, due to the slight stabilization of ketenimine **24d** by the fluorine adjacent to nitrogen. The barrier for **23d** → **24d** is still predicted to be ca. 2.5 kcal/mol higher than the barrier for **4** → **5** at the same level of theory.[48]

3.2.2.4. *ortho*-Phenyl Substituents. Alkyl, cyano, and fluoro substituents in the ortho position do not change the mechanism of phenyl azide photochemistry influencing only the rate constants of elementary reactions (k_{ISC}, k_R, k_{-R}, k_{RO}, and k_{-RO}). On the other hand, a number of photochemical and thermal cyclizations involving the ortho substituents are known for ortho-substituted phenyl azides.[9] The most interesting and important reaction of this type is formation of carbazoles **27** on pyrolysis[111] and photolysis[112] of *ortho*-biphenyl azide **26a** and a series of its derivatives.

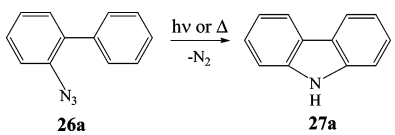

Since the early 1970s, the reactive intermediates involved in the transformation of **26a** to **27a** were studied by trapping,[113] matrix spectroscopy,[32,114] and flash photolysis.[113c,115] Swenton, Ikeler, and Williams[112] demonstrated that carbazole is derived from reaction of a singlet state species, presumably

singlet nitrene **28a**, whereas triplet nitrene **29a** dimerizes to form azo compound **30a**. Berry[115] and Sundberg[113c] studied the formation of **27a** from **26a** by monitoring the change in carbazole absorption at its maximum (289.4 nm). Carbazole was formed in cyclohexane with a rate constant of 2.2×10^3 s^{-1} at 300 K by passage over a reaction barrier of 11.5 kcal/mol.[115] Sundberg et al.[113c] obtained similar results in hydrocarbon solutions, but they found that the rate constant of carbazole formation is solvent dependent and increases to $\sim 2 \times 10^4$ s^{-1} in methanol. Since the rate constant (k_R) for cyclization of ^{1}**3** is 5−6 orders of magnitude greater than these values,[50−52] it seems unlikely that these values are actually the rate constants for formation of **27a** in a simple one-step mechanism from singlet *ortho*-biphenylnitrene (**28a**).

Indeed, the Sundberg group[113a,b] demonstrated that, in the presence of DEA, photolysis of azide **26a** leads to the formation of azepine **33a** (Scheme 6), with a concomitant

Scheme 6

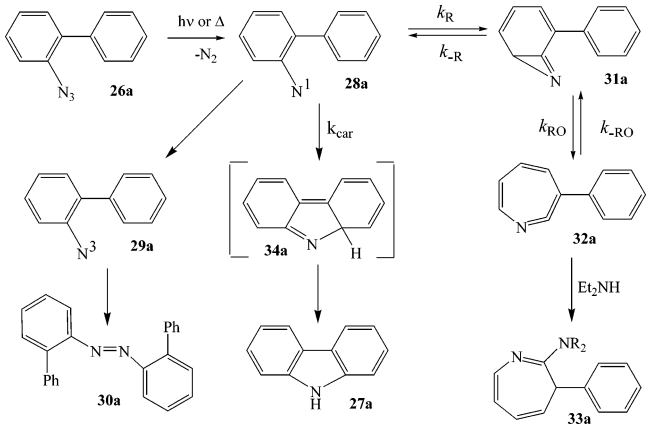

reduction in the yield of carbazole **27a**. Sundberg et al.[113] concluded that DEA traps azirine **31a** and that some **31a** must revert to singlet nitrene **28a** to explain the reduction in the yield of **23a**. Other groups have argued that **32a** is the amine-trappable species, and this hypothesis requires that the formation of both **31a** and **32a** from **28a** be reversible (Scheme 6).

Great progress has been made over the past few years[18,20,26] in understanding the photochemistry of *ortho*-biphenyl azides. The photochemistry of *ortho*-biphenyl azide **26a** has been studied by nanosecond LFP techniques with UV−Vis and IR detection of the transient intermediates and by means of quantum chemical calculations.[18] Very recently,[26] the formation and decay of singlet *ortho*-biphenylnitrene (**28a**) was detected using femtosecond transient absorption techniques. The dynamics of substituted *ortho*-biphenylnitrene, 3,5-dichloro-2-biphenylnitrene (**28b**), and products of its rearrangement were also studied by pico- and nanosecond LFP and computational methods.[20]

LFP data obtained at room temperature demonstrate that, in agreement with previous flash photolysis studies,[113c,115] **27a** is mainly formed on the millisecond time scale in pentane (Figure 15).[18] The photochemistry of **26a** was also studied by TRIR spectroscopy in acetonitrile. The characteristic ketenimine IR band of **32a** was detected at 1868 cm^{-1}. This band appeared faster than the time resolution of the apparatus (about 100 ns) and decayed on the microsecond time scale with a rate constant of $(8.3 \pm 0.8) \times 10^3$ s^{-1}. The kinetics of carbazole (**27a**) growth on this time scale was

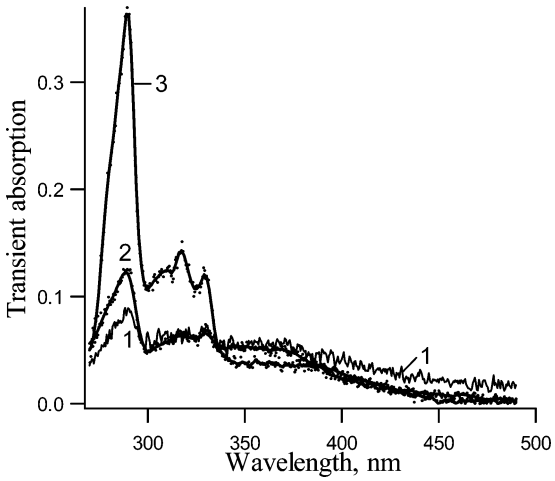

Figure 15. Transient absorption spectra detected over a window of 20 ns following LFP of *ortho*-biphenyl azide **26a** in pentane at ambient temperature. Spectra were obtained at 60 ns (1), 1 μs (2), and 5 ms (3) after the laser pulse.

monitored at 1241 cm^{-1}. The rate constant for decay of **32a** was equal, within experimental error, to the rate constant for formation of **27a** [$(11 \pm 1) \times 10^3$ s^{-1}], and both rate constants are close to the value measured by Sundberg et al. ($k = 9.8 \times 10^3$ s^{-1})[113c] for the appearance of **27a**. The TRIR experiments thus demonstrate that azacycloheptatetraene **32a** does indeed serve as a source of **27a** on the longer time scale, presumably via the mechanism shown in Scheme 6.

However, the formation of carbazole in solution is at least biphasic. In addition to the formation of **27a** on the millisecond time scale, discovered previously,[113c,115] some formation of **27a** was detected on the nanosecond time scale as well (Figure 15). The nanosecond growth of carbazole absorption at 290 nm was accompanied by the nanosecond decay of a transient absorption in the visible region between 400 and 500 nm. The time constants for the growth and decay functions are the same within experimental error and are equal to 70 ± 5 ns in pentane at ambient temperature.[18] The precursor of **27a** was assigned to isocarbazole **34a** (Scheme 6).[18]

LFP of perdeuterated azide **26a-*d*$_9$** at ambient temperature[18] demonstrated a pronounced kinetic isotope effect on the kinetics of carbazole formation on the nanosecond time scale ($k_H/k_D = 3.4 \pm 0.2$), which is consistent with the reaction being the isomerization of isocarbazole **34a** into carbazole **27a** by a 1,5-hydrogen shift. In addition, methanol and water were found to accelerate the disappearance of the transient absorption of **34a** produced upon LFP of **26a** in pentane.[18] A reasonable mechanism for this catalysis is shown in Scheme 7.

Scheme 7

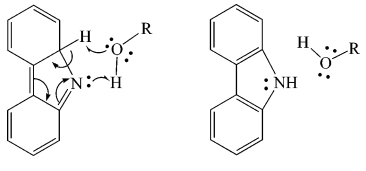

The temperature dependence of the rate constants for the decay of **34a** and **34a-*d*$_9$** in pentane were studied. At temperatures greater than 220−250 K, the data follow the

Arrhenius Law. However, the data deviates significantly from linearity below 220 K. It was proposed that this deviation from linearity involves a change in mechanism: a 1,5-hydrogen shift at higher temperature might be replaced by a catalyzed process with a lower enthalpy of activation but also with a much more negative entropy of activation.[18]

Interesting transient species was observed at 161 K (Figure 16, negative bands). This species has a strong absorption

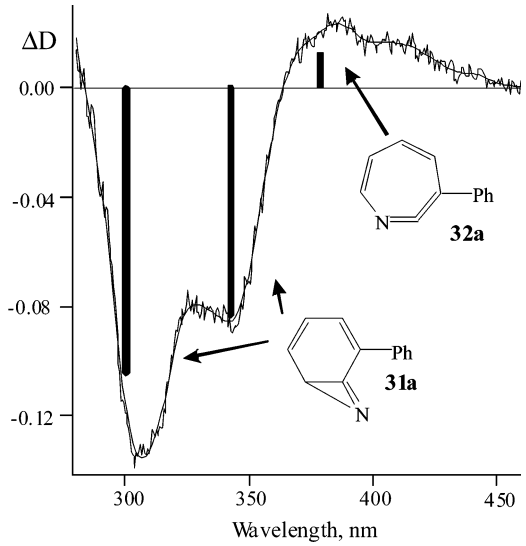

Figure 16. The difference spectrum obtained by subtracting the transient spectrum detected 4 μs after the laser pulse from that detected 150 μs after the laser pulse. The computed positions and relative oscillator strengths of the absorption bands of benzazirine **31a** and azepine **32a** are depicted as solid vertical lines (negative and positive, respectively).

band at ~305 and 340 nm and was assigned to benzazirine **31a**. Figure 16 demonstrate that the calculated spectrum of **31a** is in very good agreement with the experimental spectrum of this transient. Decay of azirine **31a** leads to the formation of a species with weak absorption at 350−400 nm, which is consistent with formation of azepine **32a** (Figure 16).[18]

In Freon-113 at ambient temperature, the lifetime of azirine **31a** is 12 ± 2 ns, which is about 6 times shorter than that for isocarbazole **34a** disappearance and carbazole **27a** formation. The temperature dependence of the observed rate constants (k_{obs}) for the decay of azirines **31a** and **31a-*d*$_9$** were studied, and the kinetic isotope effect on k_{obs} was found to be insignificant. The activation parameters were $E_{RO} = 5.7 \pm 0.1$ kcal/mol and $A_{RO} = 10^{12.1\pm0.1}$ s^{-1} for **31a** and $E_{RO} = 6.3 \pm 0.1$ kcal/mol and $A_{RO} = 10^{12.6\pm0.1}$ s^{-1} for the perdeuterated species (Table 10). The DFT calculations predict that the barrier to ring-expansion of azirine **31a** to azepine **32a** is $\Delta H^{\ddagger} = 4.7$ kcal/mol, which is within 1 kcal/mol of the experimental value of the activation energy.

As was mentioned above (Section 3.2.1), direct observations of benzazirines are rare, especially in a liquid phase. A special case is the azirine produced by LFP of 2,4,6-tri-*tert*-butylphenyl azide in pentane at ambient temperature (Section 3.2.1, Figure 12).[19]

It can be seen in Figure 15 and in the data of Sundberg et al.[113c] that there is at least one additional intermediate formed in LFP of **26a** absorbing in the range 350−450 nm. The lifetime for its decay is longer than that for azacycloheptatetraene **32a** decay and carbazole **27a** formation.[18] According to the DFT calculations,[18] isocarbazole **34a** can undergo exothermic 1,5-hydrogen shifts to form not only carbazole **27a** but also isomeric isocarbazoles **35a** and **36a** (Scheme 8). Both of these isocarbazoles were predicted to

Scheme 8

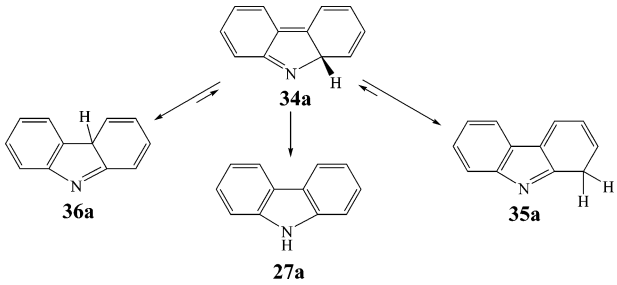

have an intense absorption around 360 nm, and it was proposed that **35a** and **36a** are responsible for the longer-lived absorptions at 350−450 nm seen in Figure 15. Presumably, subsequent 1,5-shifts in **35a** and **36a**, reform **34a**, and eventually yield more carbazole **27a**, seconds to minutes after the laser pulse (Scheme 8).[18] Therefore, formation of carbazole is not only biphasic but is most probably triphasic.

The spectrum and kinetics of singlet *ortho*-biphenylnitrene **28a** were recorded by LFP of **26a** in glassy 3-methylpentane at 77 K. It was found that singlet nitrene **28a** has $\lambda_{max} =$ 410 nm and its lifetime at 77 K is equal to 59 ± 3 ns. The perdeuterated singlet nitrene **28a-*d*$_9$** has a lifetime 80 ± 2 ns.[18]

Very recently,[26] the spectrum of singlet nitrene **28a** was detected in solution at ambient temperature using femtosecond transient absorption spectroscopy. It was found that the absorption of **28a** with maximum at ~400 nm grows with a time constant 280 ± 150 fs and decays with time constant 16 ± 3 ps. The 16 ps time constant represents the population decay time of singlet nitrene **28a** by isomerization to isocarbazole **34a** and benzazirine **31a** with the latter process being predominant. Assuming that the preexponential factor for cyclization of singlet *ortho*-biphenylnitrene **28a** is ~10^{13} s^{-1}, the activation energy could be estimated as ~3 kcal/mol.

This estimate is in excellent agreement with the predictions of (14/14) CASPT2/6-31G*//(14,14)CASSCF/6-31G* of the potential energy surface for the possible rearrangements of the singlet *ortho*-biphenylnitrene **28a** (Figure 17).[18]

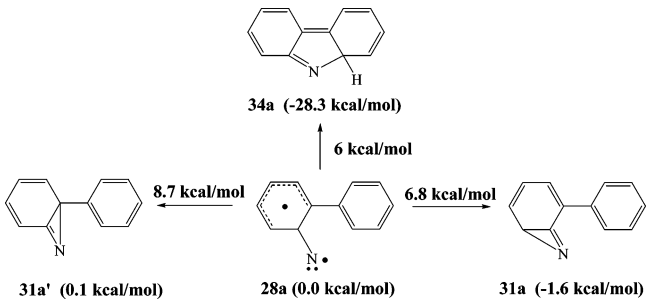

Figure 17. Structures of the intermediates formed upon cyclization of singlet *ortho*-biphenylnitrene (**28a**), their electronic energies relative to the nitrene **28a** (in parentheses), and the energy differences between the TSs and **28a**.

As shown in Figure 17, the energy difference between **28a** and the TS for its cyclization to azirine **31a** is 6.8 kcal/mol. Calculations at the same level of theory predict an energy difference of 8.5 kcal/mol between singlet phenylnitrene **13**

and the TS for its cyclization to **4**.[48] The latter energy difference is known to be too high by ~3 kcal/mol,[48] and the error in the energy difference between **28a** and the TS for its cyclization to **31a** is likely to be about the same size. Therefore, the activation energy of the cyclization of **28a** to benzazirine **31a** should be about 2 kcal/mol lower than that for parent phenylnitrene. The phenyl group lowers the enthalpy of activation for cyclization by destabilizing singlet nitrene **28a** sterically, similar to the case of *ortho*-*tert*-butyl substituent.[19]

Although the more stable of the two bicyclic azirines (**31a**) is >27 kcal/mol higher in energy than isocarbazole **34a**, the barrier to isocarbazole formation is only 0.8 kcal/mol lower than that to azepine formation. On the other hand, the TS leading to **31a** has a higher entropy than the TS leading to **34a** by 5.7 cal mol^{-1} K^{-1}.[18] At ambient temperature, the higher entropy of the TS leading to **31a** would contribute 1.7 kcal/mol to reducing its free energy. Therefore, according to the calculations both **31a** and **34a** should be formed from **28a** and azirine **31a** should be the kinetically favored product around room temperature in accord with experiment. The effective activation energy of singlet nitrene **28a** isomerization, estimated theoretically, is ~4 kcal/mol and agrees very well with the value estimated from experimental data (~3 kcal/mol).

Isocarbazole **34a** is computed to be more than 20 kcal/mol lower in enthalpy than **32a**. Therefore, unless chemically trapped, all of the **32a** that is initially formed from **28a** should ultimately isomerize to **34a** by a pathway involving ring closure of **32a** to **31a**, ring opening of **31a** to **28a**, and, finally, passage of **28a** over the TS leading to ring closure to **34a**.

Therefore, the chemistry of the unsubstituted *ortho*-biphenyl system is complicated by the fact that the key intermediate of this reaction, singlet **28a**, undergoes two cyclization processes at competitive rates and that azepine formation is reversible. It was proposed[20] that replacement of the ortho hydrogen of **28a** with chlorine atom should raise the barrier to azirine formation and not influence the barrier to isocarbazole formation. This would simplify the chemistry of singlet nitrene and allow straightforward study of the isocarbazole formation. For this purpose, 2-azido-3,5-dichlorobiphenyl azide (**26b**) was synthesized and its photochemistry was studied using nano- and picosecond transient absorption spectroscopy.[20]

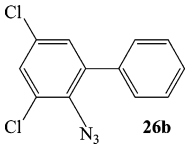

26b

At ambient temperature, LFP of **26b** in pentane produces the transient absorption spectra of Figure 18, which differ significantly from those of Figure 15. Thus, whereas unsubstituted carbazole formation takes place mainly on the millisecond time scale at ambient temperature with didehydroazepine **32a** serving as a reservoir of **28a**, the chlorinated carbazole **27b** is produced predominantly on the nanosecond time scale and only to a minor extent from the corresponding didehydroazepines **32b** and/or **32b′** (Scheme 9).

The transient absorption in the visible region (Figure 18) was assigned to a mixture of two intermediates with maxima at 470 nm and 425 and 440 nm, respectively. The lifetimes of the two intermediates differ significantly (by about 1 order

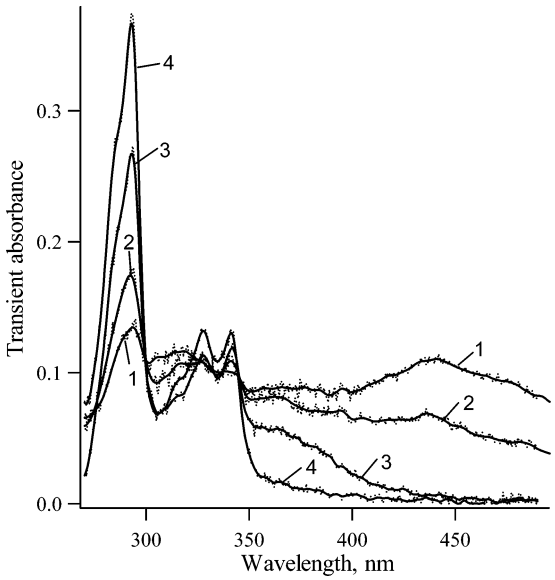

Figure 18. Transient absorption spectra detected over a window of 10 ns following LFP of 3,5-dichloro-*o*-biphenyl azide **26b** in pentane at ambient temperature 15 ns (1), 60 ns (2), 1 μs (3), and 30 ms (4) after the laser pulse.

Scheme 9

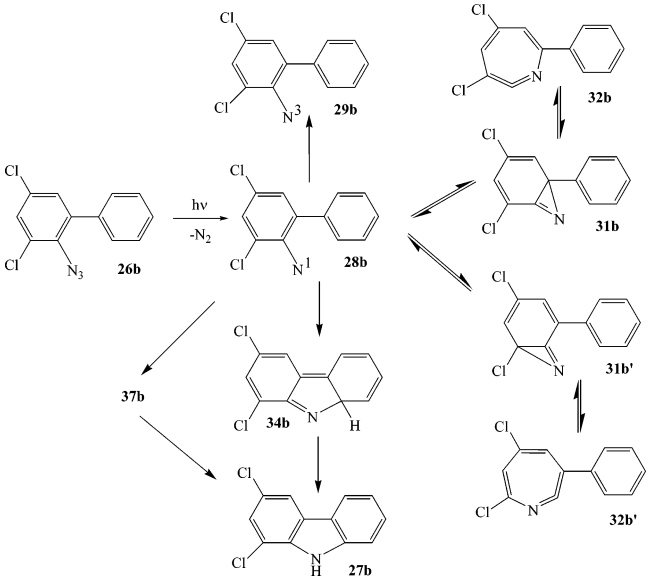

of magnitude) at 161 K, which is opposite to the case at room temperature, where they are very similar.

One of the intermediates is isocarbazole **34b** (λ_{max} = 320 and 470 nm). Its lifetime in pentane at room temperature is 65 ± 4 ns and is 263 ± 4 ns for perdeuterated analogue, similar to the case of **34a**. This intermediate (**34b**) was not detected in acetonitrile due to the acceleration of its disappearance by traces of water. Alcohols accelerate the transformation of **34b** to carbazole **27b** as well.[20]

The second intermediate (**37b**, λ_{max} = 360, 420, and 440 nm) has a lifetime at room temperature of 120 ± 10 ns in pentane, 48 ± 3 ns in acetonitrile and 53 ± 3 ns in 1-propanol. The decay of **37b** to **27b** was not accelerated by the water and alcohols. The KIE for this reaction is close to unity. Unfortunately, this intermediate was not identified.[20]

As in the case of unsubstituted *ortho*-biphenylnitrene **28a**, the transient absorption spectrum of singlet nitrene **28b** was detected at ambient temperature using a femtosecond pump−

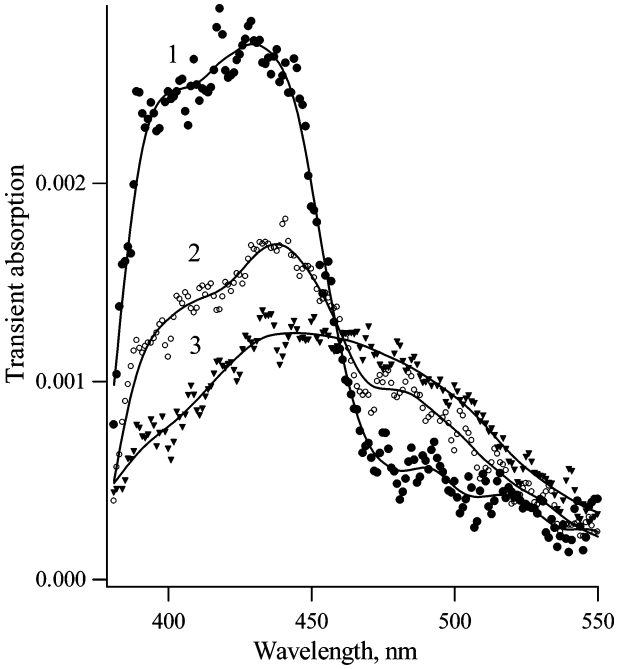

Figure 19. Transient absorption spectra recorded in pump−probe experiments (265 nm, 220 fs) upon photolysis of **26b** in cyclohexane at ambient temperature (1) 40 ps, (2) 300 ps, and (3) 630 ps after the excitation.

probe setup (Figure 19) and at 77 K by conventional LFP.[20] The spectrum detected in cyclohexane 40 ps after the laser pulse was very close to the spectrum of singlet nitrene **28b** at 77 K except for a shoulder at about 480 nm (Figure 19, spectrum 1). The decay of singlet nitrene **28b** at 420 nm was accompanied by the growth of isocarbazole **34b** with rate constant $k_{OBS} = (3.8 \pm 0.8) \times 10^9$ s^{-1} ($\tau = 260 \pm 70$ ps). It was proposed that the carrier of transient absorption detected in the region 460−550 nm 40 ps after the pump pulse is the isocarbazole **34b**, formed from a vibrationally hot state of the singlet nitrene **28b**. The rate constant for vibrational relaxation of **28b** was estimated to be $(0.9 \pm 0.2) \times 10^{11}$ s^{-1} ($\tau = 11 \pm 2$ ps).

The decay of singlet nitrene **28b** in hydrocarbon solutions was measured in three different types of experiments. The rate constant of **28b** decay (k_{OBS}) at room temperature was measured in cyclohexane using the picosecond pump−probe technique. The values of k_{OBS} were determined over the temperature range 147−167 K in pentane and at 77 K in methylcyclohexane (k_{ISC}) were obtained using nanosecond LFP. It was proposed[20] that the temperature dependence of the rate constant of the singlet nitrene decay can be described by the sum of the temperature-independent intersystem crossing rate constant (k_{ISC})[16−18,52] and the rate constant of rearrangement. The Arrhenius parameters for the rate constant of singlet nitrene **28b** rearrangement were found to be $E_a = 2.7 \pm 0.2$ kcal/mol and $A = 10^{11.6\pm0.2}$ s^{-1}.[20] These values are only effective parameters because the decay of **28b** proceeds by three different reactions with the formation of benzazirine **31b**, isocarbazole **34b**, and unidentified intermediate **37b**. Since **31b** is a minor product and the yields of **34b** and **37b** are comparable over a wide temperature range, the experimental activation energy could be compared with the calculated value of the barrier to rearrangement of **28b** to **34b**.

It was shown, using simple UB3LYP calculations,[20] that chlorine substitution (**28b**) does not influence the barrier to isocarbazole (**34b**) formation. Therefore, the barrier is predicted to be about 3 kcal/mol,[18] which is in perfect agreement with experimentally estimated activation energy for the rearrangement of the singlet nitrene **28b**.

A considerable acceleration of the singlet nitrene **28b** rearrangement was observed in methanol. The rate constant of its decay was found to be $(1.6 \pm 0.2) \times 10^{10}$ s^{-1} (62 ± 10 ps).[20] Note, that a similar, but even shorter lifetime, was measured for parent singlet biphenylnitrene **28a** in acetonitrile − 16 ± 3 ps.[26]

Unexpectedly, the yield of isocarbazole **34b** was found to depend on the energy of the photons used for the excitation of azide **26b**.[20] It drops significantly on going from excitation by a YAG (266 nm) to excimer (308 nm) laser radiation.[20] It is in line with the observation that in part the isocarbazole **34b** was formed faster than 40 ps (Figure 19), presumably from vibrationally excited singlet nitrene **28b**.

4. Photochemistry of Polycyclic Aryl Azides and Kinetics and Spectroscopy of Polycyclic Arylnitrenes

In this chapter, we will discuss the photochemistry of polycyclic aryl azides and the properties of polycyclic arylnitrenes. Fusion of a benzene ring to another aromatic ring changes the electronic structure of the nitrenes and related intermediates enough to alter their chemistry, kinetics, and thermodynamics. Polycyclic arylnitrenes can be generated by thermolysis or photolysis of the appropriate aryl azides. The photochemical and thermal reactions of polycyclic aromatic azides have been reviewed periodically,[4,7,9,116] and therefore, we will consider the early experimental results only briefly.

4.1. Early Experimental Studies

As in the case of phenylnitrene and its derivatives, the ground states of polynuclear arylnitrenes have triplet multiplicity.[33,34,117−120] This was demonstrated by the observation of the EPR spectra of triplet nitrenes in organic matrices at liquid-nitrogen temperature (Table 13).

For most polycyclic arylnitrenes, except for 2-nitrenonaphthalene, the D parameters are much smaller that of

Table 13. Zero-Field Parameters and Singlet−Triplet Energy Splitting for Arylnitrenes

nitrene	D (cm^{-1})	ref	ΔE_{ST} (kcal/mol)	ref
phenylnitrene	0.998	115	18 ± 2^a	57
			18.3 ± 0.7^a	58
			18.5^b	48
			14.8^c	60
1-nitrenonaphthalene	0.789	117	13.9^b	24
2-nitrenonaphthalene	1.008	117	16.6^b	24
	0.89	118		
	0.925	119		
1-nitrenoanthracene	0.65	120		
	0.663	117		
2-nitrenoanthracene	0.75	120		
	0.778	117		
9-nitrenoanthracene	0.47	120	5.3^b	23
			7.2^c	23
1-nitrenopyrene	0.73	34	9.8^c	60
2-nitrenopyrene		33^d	15.2^c	60
			23.0^b	60

[a] Experimentally determined. [b] Calculated by CASSCF/CASPT2 method. [c] Estimated by (U)B3LYP/6-31G* method. [d] ESR spectrum was detected, but D value was not reported.

phenylnitrene (Table 13). As in the case of phenylnitrene (Section 2.3), for polycyclic arylnitrenes one of the unpaired elctrons occupies a p-orbital on nitrogen that lies in the plane of the benzene rings and the other resides in a p-π orbital. Reduction of the *D* values is consistent with the increased delocalization of the unpaired π-electron into the π-electronic system of triplet polycyclic nitrenes, relative to phenylnitrene.

4.1.1. Naphthyl Azides and Nitrenes

Much effort has been devoted to the study of the photochemistry of 1- and 2-naphthyl azides (**38** and **39**). The products obtained upon pyrolysis and photolysis of the naphthyl azides were reported in the 1970s.[41,78,79,121−123] In 1974, the Suschitzky group[80] discovered that the thermal decomposition of **38** and **39** in bromobenzene yields a significant amount of dibenzo[a,h]phenazine (Scheme 10).

Scheme 10

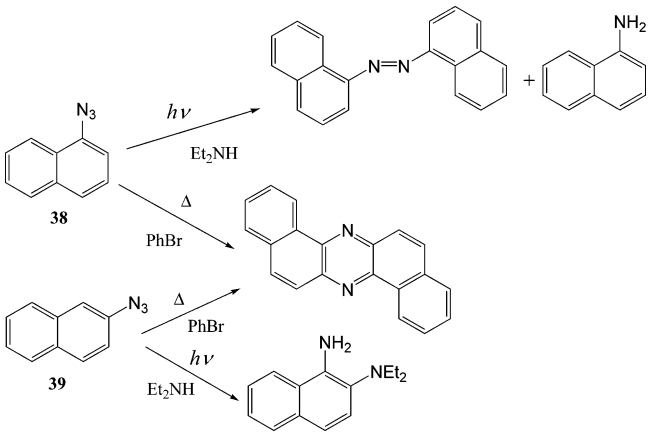

The photolytic decomposition of 2-naphthyl azide **39** in diethylamine (DEA) leads to a diamine product, but photolysis of 1-naphthyl azide **38** in DEA produces mostly azonaphthalene and aminonaphthalene in low yields[80] along with a very low yield of diamine adduct.[124]

In 1975, Carroll et al. found that the yield of diamine product is sensitive to the photolysis time.[121] A drastic reduction in photolysis time leads to a much-improved yield of the diamine. In 1977, Suschitzky's group[79] discovered that the yield of diamine products formed on photolysis of the naphthyl azides also can be significantly influenced by the presence of $(Me_2NCH_2)_2$ (TMEDA) as cosolvent. TMEDA was found to improve the yield of diamine adducts upon photolysis of both **38** and **39** in piperidine.[79] It was proposed that complexation of singlet nitrene with TMEDA suppresses ISC to the triplet nitrene.[79]

Leyva and Platz demonstrated that reaction temperature plays an important role in the photochemistry of 1-naphthyl azide,[124] similar to the case of parent phenyl azide **1**. Moderate yields of adducts were observed by simply lowering the temperature of the photolysis of **38** with DEA.

Although photolysis of **38** and **39** in the presence of secondary amine did not lead to detectable azepine products, a formal azepine adduct (**44**, Scheme 11) was observed (12% yield) upon photolysis of **38** in cyclohexylamine, a primary amine.[122] However, it has been substantiated that **44** is obtained by the trapping of azirine **41** followed by rearrangement of the initially formed adduct **43**.[123]

The photoproduct studies mentioned above, and the seminal contributions of Huisgen,[27] Doering and Odum[28] and Wentrup,[29] suggest the intermediacies of azirines and didehydroazepines in the photochemistry of 1- and 2-naphthyl azides. Additional evidence of these intermediates were provided by the observations of adducts in the photolysis of 2-naphthyl azide with ethanethiol[122] and with methanolic methoxide.[123]

Scheme 11

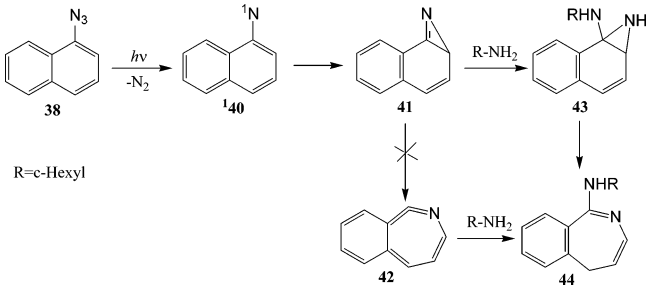

In 1980, Dunkin and Thomson obtained infrared evidence for azirines and didehydroazepines by UV-irradiation (λ > 330 nm) of **38** and **39** in nitrogen or argon matrices at 12 K.[77] In the case of **38** the IR band at 1730 cm^{-1} was formed on initial photolysis and was assigned to tricyclic azirine (**41** or **45**). The IR bands at 1926, 1912 cm^{-1}, formed on secondary photolysis of the tricyclic azirine, were attributed to didehydroazepine intermediates (**42** or/and **46**). Similarly, photolysis of **39** produces IR bands at 1708, 1723, and 1736 cm^{-1} assigned to **48** or/and **50**. The IR bands at 1911, 1923 cm^{-1} were formed on secondary photolysis and assigned to **49** or/and **51** (Scheme 12).

Scheme 12

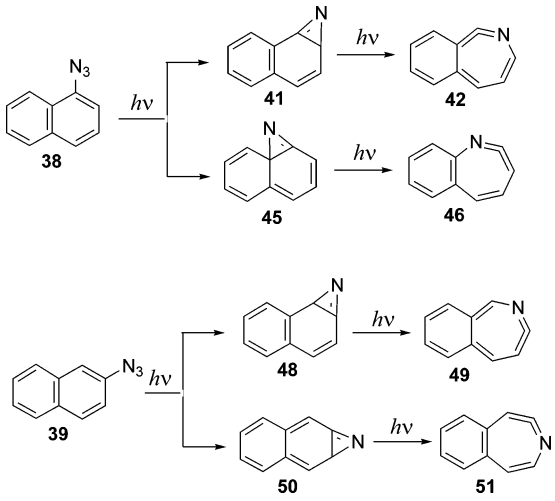

Recently,[25] photochemistry of azides **38** and **39** in argon matrix was reinvestigated, and new assignments of the experimental UV−vis and IR spectra were presented. The primary products were found to be corresponding triplet nitrenes ^{3}**40** and ^{3}**47**. According to the new assignment,[25] the peaks at 1710−1740 cm^{-1}, observed by Dunkin and Thompson,[77] belong to azirines **41** and **48**. However, the peaks at 1910−1930 cm^{-1} were assigned not to azepine **42** and **49** but to **46** and **51**. The details will be discussed in Section 4.2.

In 1984, Schrock and Schuster comprehensively examined the photochemistry of the naphthyl azides using a combination of product analysis, low-temperature spectroscopy, and LFP methodology.[33] In the case of **38**, no transient absorption above 350 nm was observed immediately after the laser flash.

However, the transient absorption spectrum of triplet nitrene (^{3}**40**, $\lambda_{max} = 370$ nm) was observed a few microseconds after the laser pulse. The intensity of the transient absorption of ^{3}**40** increased exponentially with a time constant of 2.8 μs in benzene at ambient temperature. Triplet nitrene ^{3}**40** disappeared within 100 μs accompanied by the concurrent formation of 1,1′-azonaphthalene, which absorbs strongly at 420 nm. The formation of the azo compound exhibits second-order kinetics with a rate constant of 1×10^9 M^{-1} s^{-1}. The precursor to triplet nitrene ^{3}**40** was assigned to tricyclic azirine **41** (Scheme 13), a species that serves as a reservoir

Scheme 13

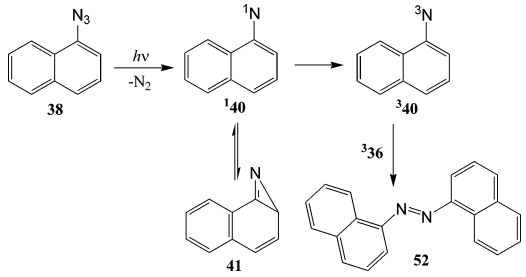

for singlet 1-naphthylnitrene ^{1}**40**. However, the latter species was not directly observed in this study.

Similar results were obtained upon photolysis of 2-naphthyl azide, **39**, except that in this case the transient absorption of triplet nitrene ^{3}**47** was too weak to permit its direct observation, and the formation of 2,2′-azonaphthalene was found to be approximately 20 times slower than that of **52**. Thus, it was concluded that the corresponding azirine **48** formed upon photolysis of **39** has a much longer lifetime than the azirine **41** produced by photolysis of **38** and that the difference in the lifetimes of these azirines is the key to understanding the profound difference in the photochemistry of **38** and **39**.[33]

4.1.2. Anthryl Azides and Nitrenes

There are three types of anthryl azides, namely, 1-, 2-, and 9-azidoanthracenes. Photolysis of these azides in organic matrices at 77 K yields the corresponding triplet nitrenes, whose electronic absorption spectra[32,44,120,125,126] and EPR spectra[117,120] (Table 13) were recorded in the 1960s.

The azo-compound was formed upon irradiation of 1-azidoanthracenes in ethanol.[32] It was formed in the reaction of triplet 1-nitrenoanthracene with starting azide with a rate constant of about 5×10^8 M^{-1} s^{-1}.

The product distributions observed upon photolysis of 2-azidoanthracene in the presence of nucleophiles resemble those formed upon photolysis of 2-azidonaphthalene[123,127] and provide evidence for the intermediacy of azirine and triplet nitrenes. To our knowledge, the photochemistry of 9-azidoanthracene in solution has not been explored by chemical analysis of reaction mixtures. The results of a recent LFP and computational chemistry study of 9-anthrylnitrene (**53**)[23] will be reviewed in Section 4.2.

4.1.3. Pyrenyl Azides and Nitrenes

The photochemistry of 1-pyrenyl azide (**54**) was studied in some detail in the 1970s[34,128−130] and reexamined in 1984 by Schrock and Schuster.[33] Irradiation of **54** in deoxygenated benzene solution gives a high yield of 1,1′-azopyrene.[33,34] When **54** was photolyzed in a diethylamine (DEA) solution with a low-power continuous light source, a large yield (82%) of 1-aminopyrene was obtained. High-power laser excitation gave a high yield of 1,1′-azopyrene and only a 4% yield of 1-aminopyrene.[33] Triplet sensitization of decomposition of **54** in benzene containing 1 M DEA at low irradiation power gave 1-aminopyrene in 55% yield.

In 1976, Sumitani, Nagakura and Yoshihara demonstrated that LFP of **54** produces a transient species with absorption maximum at 455 nm.[130] This transient absorption disappeared with a time constant of 22 ns at room temperature and 34 ns at 77 K and decayed to a species with absorption maximum at 420 nm. The intermediate with the 420 nm absorption disappeared in a second-order process to give 1,1′-azopyrene. This spectrum also was formed on triplet sensitization and was identical to that of triplet 1-nitrenopyrene (^{3}**55**) observed in a glassy matrix at 77 K. Therefore, the species with the 420 nm maximum was assigned to triplet nitrene ^{3}**55** and its precursor with maximum at 455 nm − to singlet nitrene ^{1}**55**.

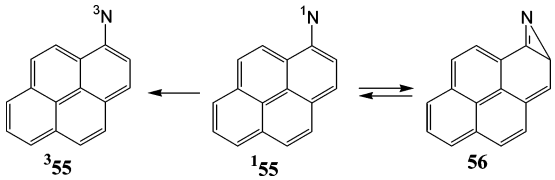

In 1984, Schrock and Schuster[33] reproduced the LFP results of Sumitani et al., but they did not exclude the possibility that the latter absorption was due to the azirine (**56**). However, in view of our recent results with phenylnitrene and its substituted derivatives,[14,16,17] it is clear that the species with absorption maximum at 455 nm is indeed singlet nitrene ^{1}**55**. Note, that until recently,[50,51] the spectrum of ^{1}**55** was the only spectrum of a singlet arylnitrene reported in the literature.

Preferential formation of triplet nitrene upon decay of ^{1}**55** is in agreement with our recent broken-symmetry DFT calculations.[60] The singlet−triplet splitting was predicted to be much smaller than that for phenylnitrene and close to the S/T gap of 9-anthrylnitrene (Table 13), which also has a rapid rate of ISC (Section 4.2).[23] In addition, cyclization of singlet nitrene ^{1}**55** to azirine **56** was predicted to be endothermic ($\Delta H_{298} = 13.8$ kcal).

The photochemistry of 2-pyrenyl azide (**57**) is quite similar to that observed for 2-naphthyl azide **39**.[33] Irradiation in benzene gives primarily 2,2′-azopyrene. In the presence of DEA, the product is almost exclusively 1-amino-2-diethylaminopyrene, and it reaches its maximum value at a very low concentration of DEA (4×10^{-3} M).

LFP of **57** produces a transient absorption with maximum at 420 nm.[33] On a longer time scale, the absorption of 2,2′-azopyrene grows by a second-order process. The 420 nm absorption band was also formed by irradiation of **57** at 77 K in glassy matrix. The EPR spectrum of triplet 2-nitrenepyrene (^{3}**58**) was detected at 77 K and at 4 K.

The same absorption band was observed in DEA as a solvent. It disappeared in a first-order process with a time constant of 2.5 μs with formation of 1-amino-2-diethylaminopyrene, absorbing at 445 nm. The authors assigned the 420 nm absorption to triplet 2-nitrenopyrene (^{3}**58**) and proposed that the conversion of singlet nitrene ^{1}**58** to its triplet ground state (^{3}**58**) is reversible.[33] However, they expressed some skepticism in this assignment.

4.2. Recent Experimental and Computational Studies

Indeed, our recent calculations[60] (Table 13) contradict the possibility of reversible conversion of ^{1}**58** to ^{3}**58**. The broken-symmetry DFT as well as more accurate CASSCF/CASPT2 calculations predict that S/T gap of nitrene **58** is close to or even higher than that for phenylnitrene **3**. Therefore, the conversion of ^{1}**58** to ^{3}**58** is irreversible.

We also performed calculations on the most interesting stationary points on the potential energy surface (PES) of singlet nitrene ^{1}**58** (Figure 20). It is seen, that this region of

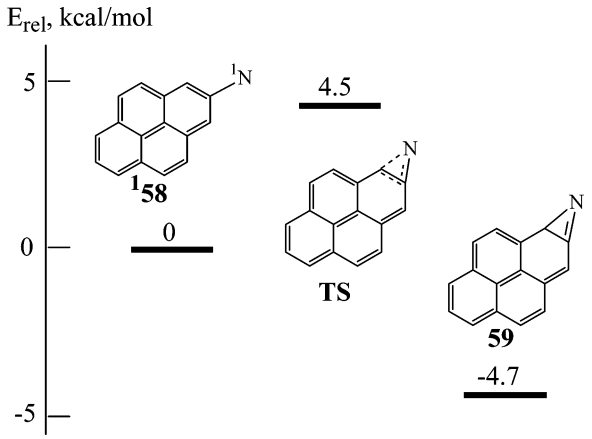

Figure 20. The relative energies of valence isomers of singlet 2-pyrenylnitrene ^{1}**58**. B3LYP/6-311+G(2d,p)//B3LYP/6-31G* energies relative to ^{3}**58** plus S/T gap from the (16,15)CASSCF/CASPT2/6-31G* calculation.

the PES is very similar to that of 2-naphthylnitrene ^{1}**47** (Figure 22), for which no triplet nitrene was detected by LFP and a long-lived azirine was observed instead.[24,33]

Moreover, time-dependent DFT calculations (TD-B3LYP/6-31+G*) predict[60] that azirine **59** has very intense absorption bands at 430 nm (f = 0.14) and 378 nm (f = 0.11). Therefore, it is most reasonable to assume that azirine **59** was detected by Schrock and Schuster[33] in their LFP experiments on the 2-pyrenyl azide **57**.

Very recently, Maltsev et al. reinvestigated the photochemistry of 1- and 2-naphthyl azides (**38** and **39**) in argon matrices.[25] This study allowed the authors to assign the UV−Vis and IR spectra of triplet nitrenes, ^{3}**40** and ^{3}**47**, azirines **41** and **48**, azepines **46** and **51**, as well as those of novel ring expansion products, the cyclic ylides **60** and **61**.

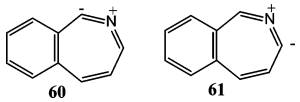

These authors also provided a comprehensive computational study of the potential energy surfaces on which the above compounds undergo their rearrangements (Figures 21 and 22).[25] It was predicted that singlet nitrene ^{1}**40** cyclizes selectively at the beta carbon with the formation of azirine **41**. The azirine derived from cyclization at carbon atom 9 is predicted to be very high in energy. Leyva and Platz[124] proposed formation of both isomeric azirines **41** and **45**, but in view of the calculations only **41** is likely to be present in solution.

Argon matrix photolysis of 1- and 2-naphthyl azides **38** and **39** at 313 nm initially affords the singlet naphthyl nitrenes, ^{1}**40** and ^{1}**47**.[25] Relaxation to the corresponding lower

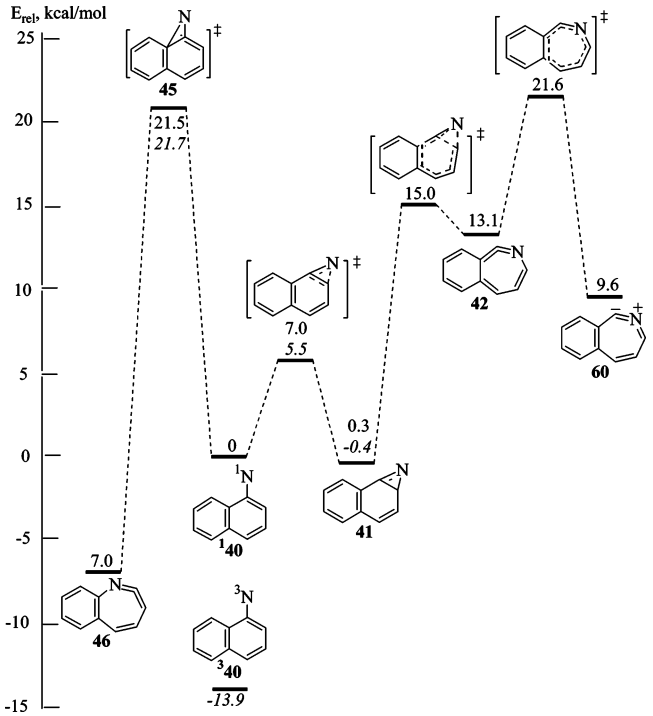

Figure 21. The relative energies of valence isomers of 1-naphthylnitrene **40**. Italic: CASPT2//CASSCF(12,12)/6-31G* energies relative to ^{1}**40**; Roman: B3LYP/6-311+G(2d,p)//B3LYP/6-31G* energies relative to ^{3}**40** plus S/T gap from the above CASPT2 calculation. All energies include zero-point energy corrections at the level used for geometry optimization. Note that **45** is a transition state by DFT but a (presumably shallow) minimum by CASSCF.

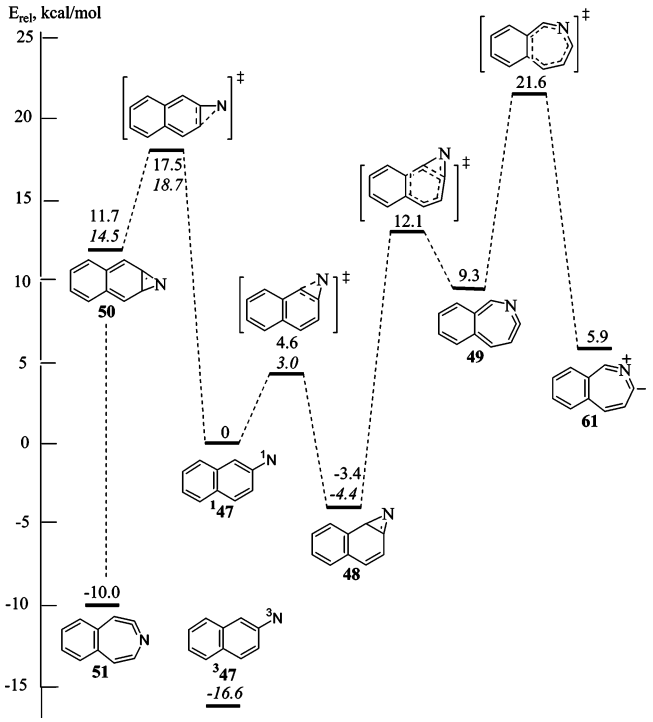

Figure 22. Relative energies of valence isomers of 2-naphthylnitrene **47**. Italic: CASPT2//CASSCF(12,12)/6-31G* energies relative to ^{1}**47**; Roman: B3LYP/6-311+G(2d,p)//B3LYP/6-31G* energies relative to ^{3}**47** plus S/T gap from the above CASPT2 calculation. All energies include zero-point energy corrections at the level used for geometry optimization.

energy, persistent triplet nitrenes ^{3}**40** and ^{3}**47** competes with cyclization to the azirines **41** and **48**, which can also be

formed photochemically from the triplet nitrenes. On prolonged irradiation, the triplet nitrenes ^{3}**40** and ^{3}**47** can be converted to the seven-membered cyclic ketenimines **46** and **51**, respectively, as described earlier by Dunkin and Thomson.[77]

However, instead of the *o*-quinoid ketenimines **42** and **49**, which are the expected primary ring-opening products of azirines **41** and **48**, respectively, the novel bond-shift isomers **60** and **61** were observed, which may be formally regarded as cyclic nitrile ylides. The existence of such ylidic heterocumulenes had been predicted previously[131] and Maltsev et al.[25] provided the first experimental observation of such species.

The electronic absorption spectra of triplet nitrenes ^{3}**40** and ^{3}**47** were detected experimentally and analyzed using time-dependent DFT and CASSCF/CASPT2 techniques.[25] Triplet nitrenes ^{3}**40** and ^{3}**47** have a moderately intense absorption in the 400−600 nm region assigned to two transitions, both involving excitation within the π system. They also have intense structured absorption bands in the near-UV region around 300−350 nm. The azirines **41** and **48** have no pronounced absorption in near UV and visible region, but they are characterized by a characteristic C=N band in the IR spectrum with 1728 cm^{-1} for **41** and 1724 cm^{-1} for **48**. The azepines **46** and **51** are characterized by a broad absorption band at about 350 nm, which are very similar to the case of **5**. The novel ylidic heterocumulenes **60** and **61** have very broad absorption bands in the visible region with maxima around 450 nm.

Recently,[24] the solution phase photochemistry of naphthyl azides **38** and **39** was reinvestigated using time-resolved IR (TRIR) techniques. LFP experiments in glassy 3-methylpentane at 77 K were performed as well. It was found that LFP of **38** at 77 K produces singlet nitrene ^{1}**40**, which is characterized by a structured band in the near-UV region with maxima at 362, 383, and 397 nm. Indeed, calculations predict that ^{1}**40** will have intense absorptions at 400, 371, 348, 342, and 315 nm as well as weak absorptions at 593 and 534 nm. All of the intense bands involve $\pi-\pi^*$ excitations.

At 77 K, the singlet nitrene ^{1}**40** relaxes to the lower energy triplet nitrene ^{3}**40** with $k_{ISC} = (1.1 \pm 0.1) \times 10^7$ s^{-1}. The cyclization of ^{1}**40** toward the β-carbon to form azirine **41** is predicted to be slightly exothermic (−0.4 kcal/mol) and to involve a barrier of 5.5 kcal/mol, according to CASPT2 calculations (Figure 21).[25] However, CASPT2 calculations were found to overestimate the barrier to cyclization of phenylnitrene by ∼3 kcal/mol.[14−17,48] If one assumes that the calculations on the naphthylnitrenes suffer from a similar error, then the barrier to cyclization of ^{1}**40** can be estimated to be ∼2.5 kcal/mol and would then be significantly smaller than that of singlet phenylnitrene ^{1}**3** (5.8 kcal/mol).[52] The experiment at 77 K reveals that the rate constant of the ^{1}**40** cyclization (k_R) is slower than k_{ISC} at that temperature. Assuming a normal *A* factor of 10^{13} s^{-1}, this result indicates that the barrier to cyclicization of ^{1}**40** must be greater than 2.1 kcal/mol. This is consistent with the 2.5 kcal/mol barrier estimated above.

In 1984, Schrock and Schuster determined the lifetime of azirine **41** to be 2.8 ± 0.2 μs by measuring the growth rate of ^{3}**40**.[33] The azirine **41** was not observed in this study because it does not absorb strongly at wavelengths greater than 300 nm.[25] The expected azirine **41** with lifetimes of 3.2 ± 0.6 μs was detected by TRIR spectroscopy.[24] The lifetime of **41** also was measured in solvent mixtures of 1:3 and 1:1 DEA/acetonitrile. The absolute bimolecular rate constants of reaction of **41** with DEA was estimated to be ∼1.4 × 10^5 M^{-1} s^{-1}, a value much smaller than that of a diffusion-controlled process. The slow rate of reaction of DEA with **41** is consistent with the reported low yield of DEA photoadduct observed upon photolysis of **38**.[80]

Unlike **38**, LFP of **39** in a glassy matrix at 77 K failed to produce a detectable transient absorption above 320 nm. Even the presumably persistent spectrum of triplet nitrene ^{3}**47** was not observed. It appears at first sight to contradict the finding of Maltsev et al.[25] that photolysis of **39** in argon at 10 K produces ^{3}**47** as a primary photoproduct. It was proposed that ^{3}**47** could be formed as a secondary photoproduct in argon at 10 K on 313 nm irradiation of **48**.[24]

The authors also proposed a second explanation to reconcile both observations.[24] It was proposed that for ^{1}**47** $k_R > k_{ISC}$ at 77 K but that $k_{ISC} > k_R$ at 12 K. If one assumes that $k_{ISC} = 1.1 \times 10^7$ s^{-1} and $A = 10^{13}$ s^{-1} for the cyclization reaction, we can conclude that the barrier to cyclization, E_a, can be bracketed as follows: $0.3 < E_a < 2.1$ kcal/mol. This result is consistent with theoretical predictions (Figure 22),[25] if the errors in CASPT2 calculations of the naphthylnitrene cyclizations are smaller than those of the singlet phenylnitrene cyclization.

Azirine **48** was detected in acetonitrile at ambient temperature using TRIR spectroscopy, and its lifetime was determined to be 150 ± 10 μs[25] in excellent agreement with Schrock and Schuster's observation of a slow rate of growth of 2,2′-azonaphthalene.[33] The long lifetime of **48** is consistent with theoretical calculations as well (Figure 22), since this azirine is predicted to be 3−4 kcal/mol more stable than singlet nitrene ^{1}**47**, whereas the cyclization of ^{1}**40** to azirine **41** is essentially thermoneutral.[25]

The rate constants of the decay were determined in the presence of 25 and 50% DEA in acetonitrile at ambient temperature. The absolute bimolecular rate constants of reaction of **48** with DEA was estimated as ∼2.5 × 10^5 M^{-1} s^{-1}. This rate constant is slightly faster but still similar to that of azirine **41** (1.4 × 10^5 M^{-1} s^{-1}).

The observed reaction of azirine **48** with DEA is not particularly fast, but trapping by DEA is still a dominant process since **48** has a long lifetime (150 μs) in the absence of the amine trap. This is consistent with the reported high yields of adducts formed upon photolysis of **39** in the presence of secondary amine.[79,80,122,123] A DEA adduct is inefficiently formed upon photolysis of **38** at ambient temperature because of the shorter lifetime of its naphthazirine derivative (**41**), which converts to ^{3}**40** in two steps and consequently renders this azirine unavailable to nucleophiles.

As was mentioned previously, the photochemistry of 9-azidoanthracene in solution has not been explored by chemical analysis of reaction mixtures. The singlet−triplet splitting of 9-anthracenylnitrene (^{1}**53**) was predicted using CASSCF/CASPT2 procedure (5.3 kcal/mol) and the simpler (U)B3LYP broken-symmetry approach (7.2 kcal/mol),[23] which is much smaller than that for parent ^{1}**3**[48] and naphthyl nitrenes ^{1}**40** and ^{1}**47**.[25] Cyclization of singlet ^{1}**53** must involve a bridgehead carbon to form an azirine intermediate **62** with

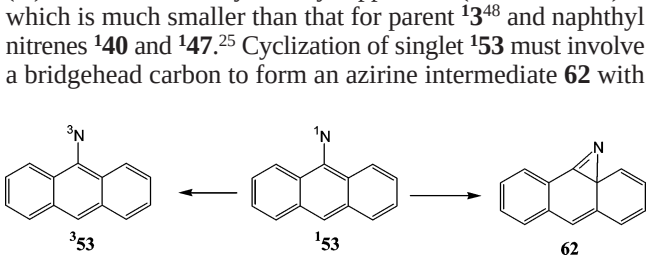

a particularly high energy. Therefore, ISC is expected to be the primary process in the decay of ^{1}**53** decay.

LFP of 9-azidoanthracene produces singlet nitrene ^{1}**53** (λ_{max} = 331, 344, and 412 nm) with reported lifetimes of 17 ns at 77 K and is 27 ns at ambient temperature. These lifetimes were the same within experimental error. Therefore, the lifetime is indeed controlled by ISC to the triplet state ^{3}**53**. The rapid rate of ISC of ^{1}**53** relative to ^{1}**3** is due to the small singlet−triplet splitting of the large delocalized nitrene. There is no evidence of cyclization of ^{1}**53** to form a bridgehead **62**. This observation is in agreement with calculations that indicate that the conversion of ^{1}**53** to **62** is endothermic by 23 kcal/mol.[23]

5. Conclusions

Study of the chemistry of aryl azides has now entered its third century. Early studies involved the synthesis of aryl azides and investigation of the chemical products they form upon thermal and then later, their light-induced decomposition. By analysis of the stable compounds produced upon activation of the azides chemists reasoned backward to deduce information about the reactive intermediates that were present during the reaction. Progress in this area was much slower than in the related field of carbene chemistry because decomposition of aryl azides often led to the formation of uninformative polymeric tar.

In the 1960s, photolysis of aryl azides immobilized in frozen organic glasses or inert gas matrices produced persistent species whose spectra could be recorded. Electron spin resonance spectroscopy was used beginning in the 1960s to identify triplet nitrenes and establish the ground-state multiplicities of aryl nitrenes. Infrared spectroscopy was used to detect cyclic ketenimines and azirines. Low temperature electronic absorption spectroscopy was of limited value because theory could provide only limited guidance to the interpretation of the experimental spectra.

With the development of nano- and picosecond LFP and advances in computational methods the chemistry of arylnitrenes has become a mature science. It is now possible to directly observe singlet arylnitrenes and follow their relaxation to azirines, ketenimines, and/or triplet nitrenes as a function of solvent and temperature. The spectra of these intermediates can be accurately simulated by theory, a tool that greatly facilitates the assignment of transient spectra. Structure−reactivity relationships have been developed, and these too are in excellent agreement with calculated barrier heights. This maturity will guide the design of a new generation of photoaffinity labeling reagents that will allow physical biochemists to find the key points of contacts between large macromolecular assemblies. New applications in other fields will surely follow as well.

New challenges await. The field of aromatic azide photochemistry is now poised to use femtosecond time-resolved methods to learn the precise details how aryl azide excited states decompose to produce singlet nitrenes and how rapidly the seminal nitrenes lose heat to solvent. We look forward to being part of this effort.

6. Acknowledgment

Support of this work by the Russian Foundation for Basic Research, Siberian Branch of Russian Academy of Sciences, and by the National Science Foundation is gratefully acknowledged.

7. References

(1) Lwowski, W., Ed. *Nitrenes*; John Wiley & Sons: New York, 1970.
(2) Breslow, D. S. In *Azides and Nitrenes; Reactivity and Utility*; Scriven, E. F. V., Ed,; Academic Press: New York, 1984; p 491.
(3) Meijer, E. W.; Nijhuis, S.; Von Vroonhoven, F. C. B. M. *J. Am. Chem. Soc.* **1988**, *110*, 7209.
(4) Smith, P. A. S. In *Nitrenes*; Lwowski, W., Ed.; Wiley-Interscience: New York, 1970; p 99.
(5) (a) Bayley, H. *Photogenerated Reagents in Biochemistry and Molecular Biology*; Elsevier: New York, 1983. (b) Bayley, H.; Staros, J. In *Azides and Nitrenes; Reactivity and Utility*; Academic Press: New York, 1984; p 434.
(6) (a) Cai, S. X.; Glenn, D. R.; Keana, J. F. W. *J. Org. Chem.* **1992**, *57*, 299. (b) Niino, H.; Koga, Y.; Yabe, A. *J. Photochem. Photobiol. A: Chemistry* **1997**, *106*, 9. (c) Niino, H.; Sato, T.; Yabe, A. *Appl. Phys. A* **1999**, *69*, 605.
(7) Scriven, E. F. V. In *Reactive Intermediates*; Abramovitch, R. A., Ed.; Plenum: New York, 1982; Vol. 2, p 1.
(8) Wentrup, C. In *Reactive Molecules*; Wiley-Interscience: New York, 1984; p 1.
(9) Smith, P. A. S. In *Azides and Nitrenes; Reactivity and Utility*; Scriven, E. F. V., Ed.; Academic: New York, 1984; p 95.
(10) Platz, M. S.; Maloney, V. M. In *Kinetics and Spectroscopy of Carbenes and Biradicals*; Platz, M. S., Ed.; Plenum: New York, 1990; p 303.
(11) Schuster, G. B.; Platz, M. S. *Adv. Photochem.* **1992**, *17*, 69.
(12) Gritsan, N. P.; Pritchina, E. A. *Russ. Chem. Rev.* **1992**, *61*, 500.
(13) Platz, M. S. *Acc. Chem. Res.* **1995**, *28*, 487.
(14) Borden, W. T.; Gritsan, N. P.; Hadad, C. M.; Karney, W. L.; Kemnitz, C. R.; Platz, M. S. *Acc. Chem. Res.* **2000**, *33*, 765.
(15) Karney, W. L.; Borden, W. T. *Adv. Carbene Chem.* **2001**, *3*, 205.
(16) Gritsan, N. P.; Platz, M. S. *Adv. Phys. Org. Chem.* **2001**, *36*, 255.
(17) Gritsan, N. P.; Platz, M. S.; Borden, W. T. In *Computational Methods in Photochemistry*; Kutateladze, A. G., Ed.; Taylor & Francis: Boca Raton, FL, 2005; p 235.
(18) Tsao, M.-L.; N. P. Gritsan, M.-L.; James, T. R.; Platz, M. S.; Hrovat, D.; Borden, W. T. *J. Am. Chem. Soc.* **2003**, *125*, 9343.
(19) Tsao, M.-L.; Platz, M. S. *J. Am. Chem. Soc.* **2003**, *125*, 12014.
(20) Gritsan, N. P.; Polshakov, D.; Tsao, M.-L., Platz, M. S. *Photochem. Photobiol. Sci.* **2005**, *4*, 23.
(21) Carra, C.; Bally, T.; Jenny, T. A.; Albini, A. *Photochem. Photobiol. Sci.* **2002**, *1*, 38.
(22) Toenshoff, C.; Bucher, G. *Eur. J. Org. Chem.* **2004**, 269.
(23) Tsao, M.-L.; Platz, M. S. *J. Phys. Chem. A* **2003**, *107*, 8879.
(24) Tsao, M.-L.; Platz, M. S. *J. Phys. Chem. A* **2004**, *108*, 1169.
(25) Maltsev, A.; Bally, T.; Tsao, M.-L.; Platz, M. S.; Kuhn, A.; Vosswinkel, M.; Wentrup, C. *J. Am. Chem. Soc.* **2004**, *126*, 237.
(26) Burdzinski, G.; Gustafson, T. L.; Hackett, J. C.; Hadad, C. M.; Platz, M. S. *J. Am. Chem. Soc.* **2005**, *127*, 13764.
(27) (a) Huisgen, R. *Angew Chem.* **1955**, *67*, 756. (b) Huisgen, R.; Vossius, D.; Appl, M. *Chem. Ber.* **1958**, *91*, 1−12. (c) Huisgen, R.; Appl, M. *Chem. Ber.* **1958**, *91*, 12.
(28) Doering, W. E.; Odum, R. A. *Tetrahedron* **1966**, *22*, 93.
(29) Wentrup, C. *Tetrahedron* **1974**, *30*, 1301
(30) Schrock, A. K.; Schuster, G. B. *J. Am. Chem. Soc.* **1984**, *106*, 5228.
(31) (a) Liang, T.-Y. and Schuster, G. B. *J. Am. Chem. Soc.* **1986**, *108*, 546. (b) Leyva, E.; Platz, M. S.; Persy, G.; Wirz, J. *J. Am. Chem. Soc.* **1986**, *108*, 3783.
(32) Reiser, A.; Willets, F. W.; Terry, G. C.; Williams, V. and Marley, R. *Trans. Faraday Soc.* **1968**, *64*, 3265.
(33) Schrock, A. K., Schuster, G. B. *J. Am. Chem. Soc.* **1984**, *106*, 5234.
(34) Yamaoka, T.; Kashiwagi, H.; Nagakura, S. *Bull. Chem. Soc. Jpn.* **1972**, *45*, 361.
(35) (a) DeGraff, B. A.; Gillespie, D. W.; Sundberg, R. J. *J. Am. Chem. Soc.* **1974**, *96*, 7491. (b) Sundberg, R. J.; Brenner, M.; Suter, S. R.; Das, B. P. *Tetrahedron Lett.* **1970**, *11*, 2715. (c) Sundberg, R. J.; Suter, S. R.; Brenner, M. *J. Am. Chem. Soc.* **1972**, *94*, 513.
(36) Shillady, D. D.; Trindle, C. *Theor. Chim. Acta* **1976**, *43*, 137.
(37) Chapman, O. L.; LeRoux, J. P. *J. Am. Chem. Soc.* **1978**, *100*, 282.
(38) (a) Donnelly, T.; Dunkin, I. R.; Norwood, D. S. D.; Prentice, A.; Shields, C. J.; Thomson, P. C. P. *J. Chem. Soc. Perkin. Trans. 2* **1985**, 307. (b) Dunkin, I. R.; Lynch, M. A.; McAlpine, F.; Sweeney, D. *J. Photochem. Photobiol. A* **1997**, *102*, 207.
(39) Shields, C. J.; Chrisope, D. R.; Schuster, G. B.; Dixon, A. J.; Poliakoff, M.; Turner, J. J. *J. Am. Chem. Soc.* **1987**, *109*, 4723.
(40) Li, Y. Z.; Kirby, J. P.; George, M. W.; Poliakoff, M.; Schuster, G. B. *J. Am. Chem. Soc.* **1988**, *110*, 8092.
(41) Warmuth, R.; Makowiec, S. *J. Am. Chem. Soc.* **2005**, *127*, 1084.
(42) Carroll, S. E.; Nay, B.; Scriven, E. F. V.; Suschitzky, H. and Thomas, D. R. *Tetrahedron Lett.* **1977**, *18*, 3175.
(43) Smolinsky, G.; Wasserman, E.; Yager, Y. A. *J. Am. Chem. Soc.* **1962**, *84*, 3220.

(44) Reiser, A.; Bowes, G.; Horne, R. *Trans. Faraday Soc.* **1966**, *62*, 3162.
(45) (a) Waddell, W. H.; Feilchenfeld, N. B. *J. Am. Chem. Soc.* **1983**, *105*, 5499. (b) Feilchenfeld, N. B.; Waddell, W. H. *Chem. Phys. Lett.* **1983**, *98*, 190.
(46) Hayes, J. C.; Sheridan, R. S. *J. Am. Chem. Soc.* **1990**, *112*, 5879.
(47) Budyka, M. F.; Kantor, M. M.; Alfimov, M. V. *Russ. Chem. Rev.* **1992**, *61*, 48.
(48) Karney, W. L.; Borden, W. T. *J. Am. Chem. Soc.* **1997**, *119*, 1378.
(49) Marcinek, A.; Leyva, E.; Whitt, D.; Platz, M. S. *J. Am. Chem. Soc.* **1993**, *115*, 8609.
(50) Gritsan, N. P.; Yuzawa, T.; Platz, M. S. *J. Am. Chem. Soc.* **1997**, *119*, 5059.
(51) Born, R.; Burda, C.; Senn, P.; Wirz, J. *J. Am. Chem. Soc.* **1997**, *119*, 5061.
(52) Gritsan, N. P.; Zhu, Z.; Hadad, C. M.; Platz, M. S. *J. Am. Chem. Soc.* **1999**, *121*, 1202.
(53) Kim, S. J. I.; Hamilton, T. P.; Schaefer, H. F., III *J. Am. Chem. Soc.* **1992**, *114*, 5349.
(54) Hrovat, D.; Waali, E. E.; Borden, W. T. *J. Am. Chem. Soc.* **1992**, *114*, 8698.
(55) Castell, O.; Carefa, V. M.; Bo, C.; Caballol, R. *J. Comput. Chem.* **1986**, *17*, 42.
(56) Smith, B. A.; Cramer, C. J. *J. Am. Chem. Soc.* **1996**, *118*, 5490.
(57) Travers, M. J.; Cowles, D. C.; Clifford, E. P.; Ellison, G. B. *J. Am. Chem. Soc.* **1992**, *114*, 8699.
(58) McDonald, R. N.; Davidson, S. J. *J. Am. Chem. Soc.* **1993**, *115*, 10857.
(59) Johnson, W. T. G.; Sullivan, M. B.; Cramer, C. J. *Int. J. Quantum Chem.* **2001**, *85*, 492.
(60) Pritchina, E. A.; Gritsan, N. P., unpublished results, 2005.
(61) Ziegler, T.; Rauk, A.; Baerends, E. *J. Theor. Chim. Acta* **1977**, *43*, 261.
(62) Gritsan, N. P.; Zhai, H. B.; Yuzawa, T.; Karweik, D.; Brooke, J. and Platz, M. S. *J. Phys. Chem. A* **1997**, *101*, 2833.
(63) Gritsan, N. P.; Pritchina. E. A. *J. Inf. Rec. Mater.* **1989**, *17*, 391.
(64) Glaiter, R.; Rettig, W.; Wentrup, C. *Helv. Chim. Acta* **1974**, *57*, 2111.
(65) Anderson, K. *Theor. Chim. Acta* **1995**, *91*, 31.
(66) Parasuk, V.; Cramer, C. J. *Chem. Phys. Lett.* **1996**, *260*, 7.
(67) Gritsan, N. P.; Tigelaar, D.; Platz, M. S. *J. Phys. Chem. A* **1999**, *103*, 4465.
(68) Gritsan, N. P.; Gudmundsdóttir, A. D.; Tigelaar, D.; Platz, M. S. *J. Phys. Chem. A* **1999**, *103*, 3458.
(69) Cerro-Lopez, M.; Gritsan, N. P.; Zhu, Z.; Platz, M. S. *J. Phys. Chem. A* **2000**, *104*, 9681.
(70) Gritsan, N. P.; Likhotvorik, I.; Tsao, M.-L.; Çelebi, N.; Platz, M. S.; Karney, W. L.; Kemnitz, C. R.; Borden, W. T. *J. Am. Chem. Soc.* **2001**, *123*, 1425.
(71) Gritsan, N. P.; Gudmundsdóttir, A. D.; Tigelaar, D.; Zhu, Z.; Karney, W. L.; Hadad, C. M.; Platz, M. S. *J. Am. Chem. Soc.* **2001**, *123*, 1951.
(72) Kobayashi, T., Suzuki, K.; Yamaoka, T. *J. Phys. Chem.* **1985**, *89*, 776.
(73) Liang, T.-Y.; Schuster, G. B. *J. Am. Chem. Soc.* **1987**, *109*, 7803.
(74) Michl, J.; Bonacic-Koutecky, V. *Electronic Aspects of Organic Photochemistry*; Wiley: New York, 1990; p 367.
(75) (a) Bonacic-Koutecky, V.; Koutecky, J.; Michl, J. *J. Angew. Chem., Int. Ed. Engl.* **1987**, *26*, 170. (b) Michl, J. *J. Am. Chem. Soc.* **1996**, *118*, 2568.
(76) Morawietz, J.; Sander, W. *J. Org. Chem.* **1996**, *61*, 4351.
(77) Dunkin, I. R.; Thomson, P. C. P. *J. Chem. Soc. Chem. Commun.* **1980**, 499.
(78) Pritchina, E. A.; Gritsan, N. P.; Bally, T. *Phys. Chem. Chem. Phys.* **2006**, *8*, 719.
(79) Carroll, S. E.; Nay, B.; Scriven, E. F. V.; Suschitzky, H. *Tetrahedron Lett.* **1977**, *18*, 943.
(80) Hilton, S. E.; Scriven, E. F. V.; Suschitzky, H. *J. Chem. Soc. Chem. Commun.* **1974**, 853.
(81) Nielsen, P. E.; Buchardt, O. *Photochem. Photobiol.* **1982**, *35*, 317.
(82) Younger, C. G.; Bell, R. A. *J. Chem. Soc. Chem. Commun.* **1992**, 1359.
(83) Polshakov, D. A.; Tsentalovich, Y. P.; Gritsan N. P. *Russ. Chem. Bull.* **2000**, *49*, 50.
(84) (a) Odum, R. A.; Aaronson, A. M. *J. Am. Chem. Soc.* **1969**, *91*, 5680. (b) Odum, R. A.; Wolf, G. *J. Chem. Soc. Chem. Commun.* **1973**, 360.
(85) Sundberg, R. J.; Suter, S. R.; Brenner, M. *J. Am. Chem. Soc.* **1972**, *94*, 513.
(86) Murata, S.; Abe, S.; Tomioka, H. *J. Org. Chem.* **1997**, *62*, 3055.
(87) Leyva, E.; Sagredo, R. *Tetrahedron* **1988**, *54*, 7367.
(88) Lamara, K.; Redhouse, A. D., Smalley, R. K.; Thompson, J. R. *Tetrahedron* **1994**, *50*, 5515.
(89) Berwick, M. A. *J. Am. Chem. Soc.* **1971**, *93*, 5780.
(90) Karney, W. L.; Borden, W. T. *J. Am. Chem. Soc.* **1997**, *119*, 3347.
(91) Abramovitch, R. A.; Challand, S. R.; Scriven, E. F. V. *J. Am. Chem. Soc.* **1972**, *94*, 1374.
(92) Abramovitch, R. A.; Challand, S. R.; Scriven, E. F. V. *J. Org. Chem.* **1975**, *40*, 1541.
(93) Banks, R. E.; Sparkes, G. R., *J. Chem. Soc., Perkin Trans. 1* **1972**, *1*, 2964.
(94) Banks, R. E.; Prakash, A. *Tetrahedron Lett.* **1973**, *14*, 99.
(95) Banks, R. E.; Prakash, A. *J. Chem. Soc., Perkin Trans. 1* **1974**, *3*, 1365.
(96) Banks, R. E.; Venayak, N. D. *J. Chem. Soc. Chem. Commun.* **1980**, *9*, 900.
(97) Poe, R.; Grayzar, J.; Young, M. J. T.; Leyva, E.; Schnapp, K. A.; Platz, M. S. *J. Am. Chem. Soc.* **1991**, *113*, 3209.
(98) Crocker, P. J.; Imai, N.; Rajagopalan, K.; Kwiatkowski, S.; Dwyer, L. D.; Vanaman, T. C.; Watt, D. C. *Bioconjugate Chemistry* **1990**, *1*, 419.
(99) Drake, R. R.; Slama, J. T.; Wall, K. A.; Abramova, M.; D'Souza, C.; Elbein, A. D.; Crocker, P. J.; Watt, D. S. *Bioconjugate Chem.* **1992**, *3*, 69.
(100) Pinney, K. C.; Katzenellenbogen, J. A. *J. Org. Chem.* **1991**, *56*, 3125.
(101) Pinney, K. C.; Carlson, K. E.; Katzenellenbogen, S. B.; Katzenellenbogen, J. A. *Biochemistry* **1991**, *30*, 2421.
(102) Kym, P. R.; Carlson, K. E.; Katzenellenbogen, J. A. *J. Med. Chem.* **1993**, *36*, 1111.
(103) Reed, M. W.; Fraga, D.; Schwartz, D. E.; Scholler, J.; Hinrichsen, R. D. *Bioconjugate Chem.* **1995**, *6*, 101.
(104) Kapfer, I.; Hawkinson, J. E.; Casida, J. E.; Goeldner, M. P. *J. Med. Chem.* **1994**, *37*, 133.
(105) Kapfer, I.; Jacques, P.; Toubal, H.; Goeldner, M. P. *Bioconjugate Chem.* **1995**, *6*, 109.
(106) Poe, R.; Schnapp, K., Young, M. J. T.; Grayzar, J.; Platz, M. S. *J. Am. Chem. Soc.* **1992**, *114*, 5054.
(107) Schnapp, K. A.; Poe, R.; Leyva, E.; Soundararajan, N.; Platz, M. S. *Bioconjugate Chem.* **1993**, *4*, 172.
(108) Schnapp, K. A.; Platz, M. S. *Bioconjugate Chem.* **1993**, *4*, 178.
(109) Marcinek, A.; Platz, M. S. *J. Phys. Chem.* **1993**, *97*, 12674.
(110) Marcinek, A.; Platz, M. S.; Chan, S. Y.; Floresca, R.; Rajagopalan, K.; Golinski, M.; Watt, D. *J. Phys. Chem.* **1994**, *98*, 412.
(111) (a) Smith, P. A. S.; Brown, B. B. *J. Am. Chem. Soc.* **1951**, *73*, 2438. (b) Smith, P. A. S.; Brown, B. B. *J. Am. Chem. Soc.* **1951**, *73*, 2435. (c) Smith, P. A. S.; Hall, J. H. *J. Am. Chem. Soc.* **1962**, *84*, 1632.
(112) Swenton, J.; Ikeler, T.; Williams, B. *J. Am. Chem. Soc.* **1970**, *92*, 3103.
(113) (a) Sundberg, R. J.; Brenner, M.; Suter, S. R.; Das, B. P. *Tetrahedron Lett.* **1970**, *31*, 2715. (b) Sundberg, R. J.; Heintzelman, R. W. *J. Org. Chem.* **1974**, *39*, 2546. (c) Sundberg, R. J.; Gillespie, D. W.; DeGraff, B. A. *J. Am. Chem. Soc.* **1975**, *97*, 6193.
(114) (a) Reiser, A.; Wanger, H.; Bowes, G. *Tetrahedron Lett.* **1966**, *23*, 629. (b) Reiser, A.; Bowes, G.; Horne, R. J. *Trans. Faraday. Soc.* **1966**, *62*, 3162.
(115) Lehman, P. A.; Berry, R. S. *J. Am. Chem. Soc.* **1973**, *95*, 8614.
(116) (a) Lwowski, W. In *Reactive Intermediates*; Jone, M., Moss R. A., Eds.; Wiley: New York, 1981; Vols. 1 and 2. (b) Wentrup, C. *Adv. Heterocycl. Chem.* **1981**, *28*, 279.
(117) Wasserman, E. *Prog. Phys. Org. Chem.* **1971**, *8*, 319.
(118) Coope, J. A. R.; Farmer, J. B,; Gardner, C. L.; McDowell, C. A. *J. Chem. Phys.* **1965**, *42*, 54.
(119) Kazaj, M.; Luerssen, H.; Wentrup, C. *Angew. Chem., Int. Ed. Engl.* **1986**, *25*, 480.
(120) Alvarado, R.; Grivet, J.-Ph.; Igier, C.; Barcelo, J.; Rigaudy, J. *J. Chem. Soc., Faraday Trans. 2*, **1977**, *73*, 844.
(121) Carroll, S. E.; Nay, B.; Scriven, E. F. V.; Suschitzky, H. *Synthesis* **1975**, 710.
(122) Nay, B.; Scriven, E. F. V.; Suschitzky, H.; Khan, Z. U. *Synthesis* **1977**, 757.
(123) Rigaudy, J.; Igier, C.; Barcelo, J. *Tetrahedron Lett.* **1975**, *16*, 3845.
(124) Leyva, E.; Platz, M. S. *Tetrahedron Lett.* **1987**, *28*, 11.
(125) Reiser, A.; Marley, R. *Trans. Faraday Soc.* **1968**, *64*, 1806.
(126) Reiser, A.; Terry, G. C.; Willets, F. W. *Nature (London)* **1966**, *211*, 410.
(127) Rigaudy, J.; Igier, C.; Barcelo, J. *Tetrahedron Lett.* **1979**, 1837.
(128) Tsunoda, T.; Yamoka, T.; Takayama, M. *Nippon Kaguku Kaishi* **1975**, *12*, 2074.
(129) Tsunoda, T.; Yamoka, T.; Osabe, Y.; Hata, Y. *Photogr. Sci. Eng.* **1976**, *20*, 188.
(130) Sumitani, M.; Nagakura, S.; Yoshihara, K. *Bull. Chem. Soc. Jpn.* **1976**, *98*, 334.
(131) Kuhn, A.; Vosswinkel, M.; Wentrup, C. *J. Org. Chem.* **2002**, *67*, 9023.

CR040055+